A SIMPLE STREAMFLOW FORECASTING SCHEME

FOR THE GANGES BASIN

A thesis

submitted by

YUDAN JIANG

In partial fulfillment of the requirements

for the degree of

Master of Science

in

Civil and Environmental Engineering

TUFTS UNIVERSITY

Department of Civil and Environmental Engineering, School of Engineering

August 2013

ADVISER:

Dr. Shafiqul Islam

ABSTRACT

This thesis develops two statistical models to predict Ganges river discharge at Hardinge Bridge in Bangladesh near India/Bangladesh border using only the previous local flow and upstream rainfall. Current operational flood forecasting in Bangladesh provides no more than 3-day lead-time forecast, matching the time it takes water in the Ganges to flow through Bangladesh, mainly due to the unreleased river flow information from India. The upstream rainfall used in this thesis is derived from freely available gridded precipitation data estimated from observed daily precipitation from the rain-gauge-observation network. The Ganges is a highly seasonal river with high discharge during July to October, and for other time the monthly mean discharge is smaller than one eighth of the critical flood level at Hardinge Bridge. Historical discharge data shows that almost all floods at Hardinge Bridge happened in August and September during the peak flow season, which is one month lagged in respect to peak season of upstream rainfall. As a result, the selected forecasting period is August-September. The first model, termed Q—Q, utilizes the persistence of previous stream flow (Q) to make predictions of future discharge. The model is able to provide promising forecasting performance within a 3-day horizon. The second model, termed Q+P—Q, combines upstream rainfall (P) with previous values of discharge to predict river flow. Results show that the Q—Q model has comparable forecast ability to Q+P—Q model within 5-day horizon, but Q+P—Q model begins to show advantage beyond 5-day horizon. For 10-day lead-time forecast, Q+P—Q model can explain 20% more variance in river discharge than Q—Q model when no rainfall forecast is included. The utility of rainfall forecast in flow predictions is also examined, model performances of 10-day lead-time flow forecast are compared when different lead-time rainfall forecasts are incorporated, and results suggest that 8-day rainfall forecast yields the best predicting capability while 6-day rainfall forecast is able to generate comparable model result.

This thesis also assesses the impact of basin scale on flow forecasting capability. Two more rivers of different drainage area are studied, Mississippi River at Clinton and Des Moines River at Keosauqua. Experiments indicate that flow forecasting capability deteriorates with the decreasing catchment size. In addition, this thesis compares hybrid model, which was proposed by Nash and Barsi (1983) and particularly developed for highly seasonal rivers, with the proposed two models in their performances. Results show that for 10-day lead-time flow forecast, Q+P—Q model outperforms hybrid model during August and September, but hybrid model provides better forecast ability than Q—Q model for whole-year forecasting.

ACKNOWLEDGEMENTS

I would like to express my deep gratitude to Dr. Shafiqul Islam for his guidance through my completion of this thesis. His profound knowledge and sharp instincts provide the unique perspective to explore this topic; his critical analyses and decisions help me conduct my research in a more effective way. I would like to thank Dr. David Small for his assistance in my MATLAB learning and his great efforts in obtaining rainfall data from a variety of sources. His comments and advice on my writing are also highly appreciated. My grateful thanks are also extended to Dr. Stephen Levine for his comments and contribution to the final version of this thesis.

I would also like to give my special thanks to Dr. Ali Shafqat Akanda for his help and encouragement through my research. Appreciation is extended to Dr. Richard Vogel and Yilan Wei for their advice in statistical modeling.

Finally I wish to thank my parents for their support throughout my study. This would not have been possible without them.

Table of Contents

1. Introduction 8
   1.1 Flood history in Bangladesh 9
   1.2 Need for flood forecasting 10
   1.3 Current situation of flood forecasting in Bangladesh 11
   1.4 Flood forecasting horizon 13
2. Prior efforts in Bangladesh flood forecasting 15
   2.1 Ensemble flood forecasting review 15
   2.2 Prior efforts in Bangladesh Flood forecasting 16
3. Ganges Floods and Rainfall-Runoff Relationships 22
   3.1 Ganges basin and flood history 22
   3.2 Temporal and spatial distribution of rainfall over Ganges basin 25
   3.3 Rainfall-Runoff relationship 26
4. A Simple Q—Q and Q+P—Q Model for Ganges 29
   4.1 A Persistence based Q—Q model 29
   4.2 A simple Q+P—Q model 31
   4.3 Adding the 'perfect rainfall forecast' 33
5. Impact of basin scale on forecasting ability: application of hybrid model 36
   5.1 Introduction to hybrid model 39
   5.2 Comparisons of model performance between Q+P—Q model and hybrid model 40
   5.3 Comparisons of model performances among three basins 41
6. Results and Discussion 43
   6.1 Comparing Q—Q and Q+P—Q model 43
   6.2 The utility of rainfall forecast 44
   6.3 The impact of basin scale on forecasting ability 45
7. APPENDIX 46
8. REFERENCES 60

LIST OF TABLES

Table 1 Flood situation during 1951-2007 24

Table 2 Peak situation in normal years during 1951-2007 24

Table 3 P—Q correlation (1951-2007) 28

Table 4 Model performance for Aug/Sep flow of validation period (1991-2007) 31

Table 5 Comparisons of two models for validation period (1991-2007) 33

Table 6 Model results for different rainfall lead-time of validation period (1991-2007) 34

Table 7 Autocorrelation function for three basins (whole-year) 39

Table 8 Comparison of Q—Q model performances for three basins (whole-year) 40

Table 9 10-day lead-time flow forecasting results of different models for Aug/Sep on Ganges . 41

Table 10 Hybrid model results for 5-day and 10-day lead-time forecast (whole year) 42

LIST OF FIGURES

Figure 1 Ganges-Brahmaputra-Meghna (GBM) system and Bangladesh (Akhtar et al., 2009) 10

Figure 2 Hardinge Bridge (HB) on Ganges and Bahadurabad (B) on Brahmaputra (Jian et al., 2009).... 14

Figure 3 Monthly mean discharge at Hardinge Bridge and basin-average precipitation over Ganges basin 25

Figure 4 Travel-time-based domain division for Ganges basin. 26

Figure 5 Forecasted discharge (10-day lead-time flood forecast with 6-day lead-time 'perfect rainfall forecast') 35

Figure 6 Monthly mean discharge and precipitation for three basins. 'Q' and 'P' denote discharge and basin-average precipitation. 38

1. Introduction

As the third largest freshwater outlet to ocean globally, the discharge of the Ganges-Brahmaputra-Meghna (GBM) system is only exceeded by the Amazon and the Congo Rivers (Chowdhury and Ward, 2004). The drainage area for Ganges, Brahmaputra and Meghna is 907×10^3 km^2, 583×10^3 km^2 and 65×10^3 km^2, respectively. The Ganges originates in the southern foothills of the Himalaya Mountains in India, flowing 2000 km before entering Bangladesh from the west and flowing southeast for 250 km to join Brahmaputra (Rasid and Paul, 1987). The Brahmaputra rises from Chinese side of Himalaya, flows through Tibet and India for 1800 km and enters the northern side of Bangladesh, then meets Ganges after traveling for another 275 km. Together, they make one of the widest river channels in the world, ranging between 10 km and 20 km with an average floodplain along the river between 25 and 35 km wide. Meghna originates from one of the rainiest hillslopes in the world, meanders through India for about 400 km and enters northeast Bangladesh, then flows through its confluence and joins Ganges on the way. The lower Meghna has a comparable dimension to Ganges and Brahmaputra.

Bangladesh is located at the confluence of the three major rivers (Fig.1), but occupies only 8% of its total drainage area (Jakobsen et al., 2005). It is considered to be the most flood-affected country in the world, with at least one fifth of its area inundated by flood waters every year and as much as two thirds inundated during extreme events (Mirza et al., 2001). Because Bangladesh is very flat, with an elevation gradient from the coast northward of 1m per 50km, once the water level exceeds flood stage, floodwaters could quickly spread out across the extensive floodplain (Webster et al., 2010). The flatness also contributes to the stagnation of flood waters, and impedes the recession of excess water during high floods (Rasid and Paul, 1987).

River flow within Bangladesh is mainly generated by rainfall over the huge GBM drainage area outside of the country, intensive rainfall over this area would cause flooding in this country, while

local rainfall becomes less dominant (Chowdhury and Ward, 2007). When upstream GBM basins receive increased amount of rainfall, there exists high risk of flood for downstream (Bangladesh); However, if Bangladesh also receives heavy rainfall, the chance of getting an extreme flood is even higher, as is the case in 1987 (Brammer, 1990) .

1.1 Flood history in Bangladesh

Almost all of Bangladesh sits within the tropical monsoon climate region, according to Koeppen's classification system (Rasid and Paul, 1987). This brings highly seasonal rainfall to the country. The upstream region of the GBM basins also receive highly seasonal rainfall; for example, over upstream Ganges basin, annual average rainfall during 1951-2007 was 847 mm, 87% of which occurred during monsoon season (June to September). Flooding is an annual recurring event during monsoon season in Bangladesh, and since 1954 roughly 18% of Bangladesh has been inundated every year (Chowdhury, 2003). However, the floods were usually short-lived and not always caused adverse impacts to agriculture and society due to sufficient irregularity (Jian et al., 2009).

Major flooding events occurred in Bangladesh with a return period of 4-5 years (Hopson and Webster, 2010). Hossain et al. (1987) reported serious floods in 1954, 1955, 1956, 1962, 1963, 1968, 1970, 1971, 1974 and 1984 in Bangladesh. Three recent extreme floods occurred in 1987, 1988 and 1998, with 36%, 63% and 69% of Bangladesh inundated, respectively (Mirza, 2003). Webster et al. (2010) explained that the three tremendous floods were caused by the synchronization of peaks on Ganges and Brahmaputra, and the situation was even worse in 1998 compared to the other two years, when sea level rose by 30cm at the head of the Bay of Bengal and thus restricting river outflow. In recent decade, the Brahmaputra flooded large area of Bangladesh in 2004 and 2007 (Jian et al., 2009).

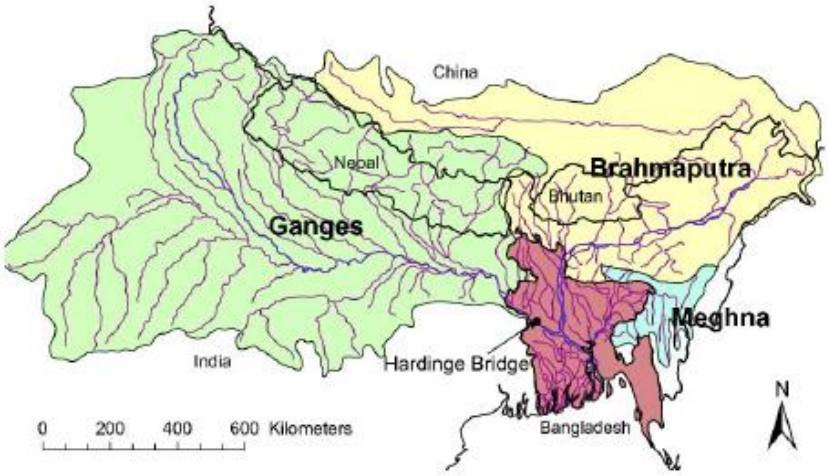

Figure 1 Ganges-Brahmaputra-Meghna (GBM) system and Bangladesh (Akhtar et al., 2009)

1.2 Need for flood forecasting

The flood-prone area in Bangladesh makes up 42% of the country's geographical area, and the loss caused by floods is tremendous (Mirza, 2001). In a normal year, Bangladesh suffered a loss of US $175 million while it increased to $2 billion in extreme cases.

Rasid and Paul (1987) suggested that the commonsense way to prevent flood damage is floodplain regulation, and that the key to its success is the sufficient delineation of flood hazard area. However, approximately 10% of Bangladesh is water body, and due to the lack of land resources, relocating floodplain population is not feasible. More than one-third of the population in this country has to live on 100-year floodplains, which is the basis of flood-prone area delineation (Whipple et al., 1983). In addition, engineering solutions in terms of flood control projects in Bangladesh seem to have limited achievements, as designing adequate structures is difficult for such complex river systems, plus multi-basin projects require mass investment which the country could not afford (Rasid and Paul, 1987). As another nonstructural measure, timely flood forecasting and warning is viewed as a key way to reduce flood damages, and it is also highly cost-effective (Chowdhury, 2000). To

help residents evacuate and secure their property ahead of time, the warning provided by a reliable forecasting system is critical.

Flood forecasting is also essential for agriculture planning to minimize loss in agricultural inputs (seed, fertilizer, pesticides). As an agrarian country, Bangladesh relies on floods in its agricultural practices (Chowdhury and Ward, 2007). However, the agriculture in Bangladesh is both flood dependent and flood vulnerable (Rasid and Paul, 1987). That is, in normal years flood brings adequate moisture and fertilizer to support crop growth, but in abnormal years, flood significantly decreased crop production in certain areas. Though extreme events impeded food production in flood-affected areas, the above-average rainfall benefited crops outside the area, as Montgomery (1985) found that total production of aman, one of the major agricultural crops in Bangladesh (Rahman et al, 2004), was usually higher in high flood years. Besides, the timing of flood is quite important, as it plays a critical role in winter rice harvest, summer rice planting, and deciding the viability of planting other crops throughout the year (Webster et al., 2010). Take aman for example, it is planted in June-July and harvested in September-October, both periods occurring during the monsoon season. Therefore, timely flood forecasting could provide valuable strategies for agriculture practices.

1.3 Current situation of flood forecasting in Bangladesh

As the drainage basins of GBM system mainly lie outside of Bangladesh, traditional methods of flood forecasting in Bangladesh would require the cooperation from its upstream neighbor India to provide flow data. However, currently this data is not available, and the only data available is water level measured by Bangladesh authorities on the rivers within Bangladesh, and at some gauging stations where rated discharge is available, river discharge is calculated. The most upstream stations with rated discharge are Hardinge Bridge for Ganges and Bahadurabad for Brahmaputra. (Fig. 2) To Bangladesh, unreleased upstream data makes the two rivers residing outside of Bangladesh as two

largest un-gaged rivers in the world. This results in a maximum of 3-day lead-time flow forecasting within Bangladesh, the time it takes water to flow through the country in the two rivers before exiting to Bay of Bengal.

The Flood Forecasting and Warning Center (FFWC) was established in 1972 under the administrative control of the Bangladesh Water Development Board (BWDB) to assist national preparedness for floods (Chowdhury, 2000). Jakobsen et al. (2005) pointed out that according to Paudyal (2001) the FFWC generates flood warnings during the flood season for monsoon river flood, local rainwater flood and flash flood, but not for storm surge flood. Every day, 24, 48 and 72 h forecasts are made in Bangladesh at 30 forecasting stations (Chowdhury, 2007). Real-time local precipitation and river conditions are essential for forecasting, as well as adequate simulation of rainfall-runoff process and river flow in the channel. For this purpose, a general numerical hydrodynamic model system MIKE 11 developed by Danish Hydraulic Institute (DHI) has been incorporated into the flood forecasting system since 1992. The model is presently named as FF2003 Model and utilizes topography information of Bangladesh (Jakobsen et al., 2005).

During flood season, FFWC estimates water level at Pankha and Noonkhawa, where Ganges and Brahmaputra enters Bangladesh from India, for 24, 48, and 72-hr lead-time.[1] This is mere subjective judgment, using the current water level, satellite estimate rainfall over upstream Ganges basin and upstream water level in India if it is available). These estimates are then used as boundary conditions in MIKE 11 to forecast water level for downstream stations up to 3-day lead- time. This is the conventional forecast being used in Bangladesh, named 3-day deterministic flood forecast on FFWC's website (http://www.ffwc.gov.bd/). To replace the subjective judgment in determining the water level near India/Bangladesh border, Webster et al.(2010) applied ensemble probabilistic forecast to predict water level at Hardinge Bridge and Bahadurabad for 1-10-day horizon. Three sets

[1] Knowledge in this paragraph is gained from conversations with Wahid Palash, a hydrodynamic modeler and water specialist in Bangladesh.

of data, mean, upper bound (mean + 1*std.dev) and lower bound (mean - 1*std.dev), are then used as boundary conditions for MIKE 11 to run forecasts for other stations within the country. However, this approach is still at experimental stage, and the results are disseminated to public only via FFWC website. In addition, according to the website, a 5-day deterministic flood forecast is also being at experimental stage.

1.4 Flood forecasting horizon

Bangladeshi Center for Environmental and Geographic Information Services (CEGIS, 2006) estimated that 2-day forecast could only reduce post-flood households and agricultural costs by 2% while 7-day forecast could reduce by 20% (Webster et al., 2010). Asian Disaster Preparedness Center (ADPC, 2002) noted that the minimum forecast horizon that allows farming community to take effective actions against flood/drought is about 10 days, and optimal period is in excess of 3 weeks (Webster and Hoyos, 2004). In order to extend the forecast horizon within Bangladesh, an effective forecasting system at India/Bangladesh border must be established to replace the current subjective judgment estimation and therefore extend forecast lead-time for other river stations within the country.

Webster et al. (2010) described a basic strategy for an overlapping tiered flood forecasting system for Bangladesh, which is proposed during an exploratory project Climate Forecast Applications in Bangladesh (CFAB)[2]. The forecasting periods consist of seasonal, intermediate and short-term, each of which has a horizon of 1-6 months, 15-30 days and 1-10, 1-15 days. Seasonal forecast is valuable in selection of crops and seed varieties, early preparation for disasters as well as possibly mitigation; intermediate forecast can enable tactical adjustments to already-made strategies based on seasonal forecast; and short-term forecast is capable of providing timely guidance to

[2] CFAB is funded by U.S. Agency for International Development's Office of Foreign Disaster Assistance (USAID-OFDA) to provide advanced flood warning in Bangladesh on daily to seasonal timescales.

residents in terms of evacuating and securing the properties (grain stores, livestock, and other economic assets).

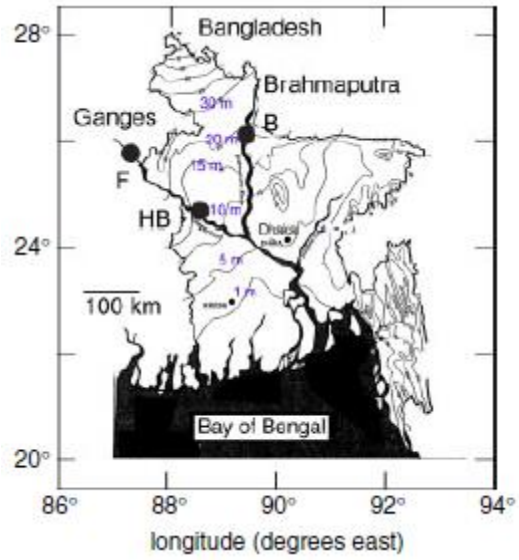

Figure 2 Hardinge Bridge (HB) on Ganges and Bahadurabad (B) on Brahmaputra (Jian et al., 2009)

2. Prior efforts in Bangladesh flood forecasting

2.1 Ensemble flood forecasting review

Lately, the hydrological community is increasingly interested in ensemble flood forecasting, which incorporates ensembles of numerical weather predictions (NWP) instead of single deterministic forecasts to make predictions (Thielen et al., 2009). Cloke and Pappenberger (2009) reviewed published case studies on ensemble flood forecasting, and found that the majority are based on single hindcasted events, while only a few have evaluated multiple events over several years. It is also clear that the majority of studies are on small rivers and that large rivers have rarely been studied, except for Ganges and Brahmaputra (Webster et al., 2010), which is discussed later.

Cloke and Pappenberger (2009) came across several studies suggesting added value in ensemble flood forecasting compared to single deterministic forecasting. There is also evidence that ensemble flood forecasting greatly relies on the accuracy of quantitative precipitation forecast generated by meteorological models, in respect to the timing, intensity, amount and spatial distribution. Though the weather prediction abilities have steadily improved over the past years due to higher resolution models, better measurements and advanced data processing methods, the ability in predicting intense rainfall remains low and has barely increased (Thielen et al., 2009). Despite the sensitivity of flood forecast on precipitation inputs in some cases, the general agreement in literature is that ensemble flood forecast is useful in issuing early flood warning. For example, Pappenberger et al. (2008) addressed that incorporation of NWP can significantly increase flood forecast lead-time.

As the full set of 7 global ensembles in the THORPEX Interactive Grand Global Ensemble (TIGGE) data archive became available in 2007 (Pappenberger et al., 2008), a new direction in early flood warning emerged using grand-ensemble weather predictions, which merges ensembles from 7 forecast centers worldwide. Case studies on Jiu river, one of tributaries to the Danube in Romania, and Upper Severn catchment in the Midlands region of England both illustrate that grand-ensemble

forecast is a promising approach in issuing early flood warning (Pappenberger et al., 2008; He et al., 2009).

Cloke and Pappenberger (2009) also reported key challenges in using ensemble flood forecast, some of which are discussed here. First, the NWPs are not good enough and for example improvement on its resolution and number of ensembles is needed. Second, as extreme floods are rare events, there are not enough instances to adequately calibrate models or evaluate their performance, plus most studies tend to avoid reporting failure (false alarm) of their particular system. Third, the intensive demand for computer power might restrict the use of ensemble methods in operational systems, especially for the case of the recently proposed grand-ensemble forecast which further burdens computation by increasing the number of ensemble members. Fourth, it remains a challenge that how to interpret the forecasting result, how to incorporate it into the decision support system and how to best communicate it with the end users. In addition, no matter it is hindcast or real-time forecast, the model performance evaluation tends to be quite subjective. Therefore, there is a need to establish a scoring system for general assessment in these studies.

2.2 Prior efforts in Bangladesh Flood forecasting

As addressed earlier, upstream river flow data on Ganges and Brahmaputra within India is not shared between India and Bangladesh, hence it is essential to establish a flood forecasting system at India/Bangladesh border to extend forecast horizon within Bangladesh. Therefore, Bangladesh flood forecast studies mainly focus on predicting Ganges discharge at Hardinge Bridge and Brahmaputra discharge at Bahadurabad, both near India/Bangladesh border. They are not the points where the two rivers enter Bangladesh, however, they are the farthest upstream locations with available rated discharge. As a result, they are used as boundary conditions so that the estimated discharge could be verified.

Hopson and Webster (2010) described a fully automated scheme for 1-10 day lead-time flood forecasting at Hardinge Bridge and Bahadurabad during 2003-2007. European Center for Medium-Range Weather Forecasts (ECMWF) ensemble prediction schemes were adopted, and the meteorological model output was calibrated using the precipitation inputs from National Aeronautics and Space Administration (NASA) and National Oceanic and Atmospheric Administration (NOAA) to reduce system errors. Results suggested that expect for moderate forecast ability in 2003, all major floods were well forecasted at 10-day lead-time during 2003-2008 for Brahmaputra. Overall, the timing of flood (the onset and end of the flood period) and forecast flood risk probabilities were skillful, despite that the peak magnitude might be either noticeable overestimated or underestimated at times. For Ganges, forecasts were less skillful. There were no severe floods on Ganges at Hardinge Bridge during the study period. They suggested that for Ganges, forecasts begin to lose value after 5-day lead-time and argued that one reason was that water management of Ganges was not appropriately incorporated into the forecast system.

Webster et al. (2010) extended the forecast to 2009 for both rivers. In 2009 no flood occurred in Bangladesh in either rivers and none was forecasted, but moderate flood risk probabilities were forecasted during late August/early September on Brahmaputra. Compared to their work discussed earlier, they introduced several metrics to assess the results. Ensemble mean was mainly used to evaluate the performance, and correlations between ensemble mean and observation for different lead-time were calculated. Brier score, which aims to assess the accuracy of probability forecast, was used. And to compare with reference (persistence) forecast, Brier skill score was also introduced. They also evaluated the contributions of ECMWF quantitative precipitation forecast (QPFs) to the forecast system, and their Table 4 suggested that the value of QPFs became evident after 5-day lead-time forecast. In addition, they increased the lead-time to 15- and 30-day since 2008 for both rivers. For 15-day lead-time forecast, positive bias was detected in all cases, and they suggested to extend the operational forecast to 15-day with necessary future work. For 30-day lead-time forecast, they

referred to Vitart (2004) and suggested that little clustering of ensemble members existed for this horizon, and thus reported little value using the present forecast system.

The advantage of their work is, within 10-day lead-time, the observed discharge is generally contained within the ensembles spread, the forecast scheme displays capability in capturing the onset and end of flood period, and high flood risk probabilities were forecasted most of the time during flood period. It suggests that the forecast system has the capability of representing total uncertainty. However, the challenge would be how to interpret the ensemble forecasting results and issue effective warning, how to utilize it to make predictions for other river stations within the country, and ultimately how to communicate with the user community and provide with proper guidance.

In recent years, researchers have been exploring alternative approaches for Bangladesh flood forecasting, as discussed in the following paragraphs. For example the artificial neural network has been applied as a statistical tool to capture the flow data pattern and thus making predictions. Besides, remote sensing techniques have also been employed for river discharge predictions, some directly use related satellite data for water elevation estimation, some incorporate other data (snow, surface soil moisture) derived from this technique to improve flow forecasting. However, the progress made are still limited.

Akhtar et al. (2009) applied artificial neural network (ANN) in Ganges flow forecasting. The study period is 2001-2005, with 2001-2003 for training and 2004-2005 for verification. The input variables consist of previous river flow, previous lagged area-average rainfall, sum of lagged rainfall and actual evapotranspiration (AET), and they were grouped into four options in the study. As they noted that low flow was less dominated by previous upstream rainfall but more by local groundwater dynamics, only high flow was selected for the analysis as the goal was to build flood forecast model. Experiments suggested that within 5-day forecast horizon, rainfall and AET failed to add value compared to the persistence forecast (only previous flow used as input), and sum of lagged rainfall seemed to produce better results than lagged area-average rainfall when combined with previous

flow as inputs. They conducted experiments up to 10-day lead-time, and results showed that the value of rainfall (sum of lagged rainfall as input) started to become evident beyond 7-day. It is worth mentioning their use of flow length and travel time as an approach to incorporate spatial precipitation into the ANN model. As Ganges runs through such a large scale basin, the spatial distribution of precipitation could be critical in predicting river flow at Hardinge Bridge. The disadvantage of this work is that the ANN model structure is unknown, and for statistical methods the training period is considered short.

Biancamaria et al. (2011) utilized Topex/Poseidon satellite altimetry measurements in India on Ganges and Brahmaputra to estimate water elevation anomalies at Hardinge Bridge and Bahadurabad. They reported good quality forecast for 5-day lead-time, and suggested that although 10-day lead-time forecast yielded higher errors but could still be valuable in operational forecast. However, there exist several limitations for this approach. First, historical long record of satellite altimeters data is not available, thus restricting long-term study within this framework (less than 2-year data was used in this study). Second, as the current generation satellite altimeters were primary designed for oceanographic purposes, the low time resolution (10-day repeat period in this study) and relatively inaccurate river heights measurement remain an issue. In addition, to realize real-time forecast, additional efforts are a must to shorten the repeat period, and the combined use of different satellite products might become promising to improve forecast performance. And they also addressed that the future Surface Water and Ocean Topography (SWOT) wide swath altimeter would provide improved forecast coverage and accuracy, and would be able to solve the problem.

Hirpa et al. (2013) employed passive microwave sensing technique at more than 20 locations upstream of Hardinge Bridge and Bahadurabad for river discharge nowcasting and forecasting at these two specific gauging stations. For different lead-time, the maximum correlation between satellite-derived flow (SDF) and gauge discharge observations was selected as the basis for forecasting. The SDF forecast tended to underestimate the peaks for both rivers, especially for

Brahmaputra, but showed capability in capturing the rising and recession limbs of the hydrograph. After combined with 'persistence forecast', the forecast performance was greatly improved; for Brahmaputra the forecast had considerably better performance than autoregressive moving-average (ARMA) model beyond 3-day horizon, but for Ganges the forecast was slightly worse than ARMA model up to 10-day. However, they argued that the weakness of using ARMA model was that the continuous past observations must be available, and thus their approach still provided useful perspectives.

Siddique-E-Akbor et al. (2011) compared water level estimates obtained from two methods, Envisat satellite altimetry and hydrodynamic-hydrologic (HEC-RAS) model, for three rivers in Bangladesh. They reported that in general the average root mean square error (RMSE) was larger than 2.0 m, and Brahmaputra had both the lowest RMSE (0.67m) and highest correlation (1.00). As the HEC-RAS model simulated estimate had relatively lower RMSE (0.7-1.2m), they suggested that the model estimates might be an alternative benchmarking inland altimetry data when in-situ gauging observations were not available.

Some studies use remote sensing techniques to improve forecast of single component (snow, surface soil moisture) in flood model, and reported its potential in flood forecasting. Bindlish et al. (2009) demonstrated the potential of utilizing remotely sensed surface soil moisture data in improving streamflow forecasting for a catchment of 236,985 km^2 during a flood event in northeastern Australia, and suggested that the potential was particularly high for catchments lacking good river flow and ground-based rainfall measurements. Dechant and Moradkhani (2011) also concluded that remotely sensed microwave radiance data showed potential in snow water equivalent prediction and thus benefited streamflow forecasting. However, according to the author's knowledge, there are no similar studies for large basins like Ganges and Brahmaputra, probably due to the large scale of the basin.

All of the studies mentioned above only include short-period study, and the only statistical approach used ANN model but didn't come up with a specific model. Therefore, to fill in this gap, simple statistical models with long-term study are proposed in this thesis.

3. Ganges Floods and Rainfall-Runoff Relationship

This thesis only focuses on the Ganges, and the goal is to develop a flood forecasting system at Hardinge Bridge, near India/Bangladesh border. In this section, historical records of daily discharge on the Ganges at Hardinge Bridge and daily precipitation over upstream Ganges basin are analyzed to discuss the pattern of flood period and the relationship between rainfall and river discharge. The river discharge at Hardinge Bridge was calculated from water level measurements by Bangladesh authority during 1934/4/1-2009/3/30, with missing records during 1971/3/21-1972/3/31 and 1999/10/28-1999/10/31. The precipitation data was generated by APHRODITE's Water Resources project[3], in daily timescale with different spatial resolution, created primarily with data derived from rain-gauge-observation network. 0.5-degree-grid data is selected considering the basin size. The precipitation data is available from 1951 to 2007, with values below 10^{-7} (mm) rounded to zero. It is observed that historically flood level was only exceeded at Hardinge Bridge during 8/14-10/10, with overwhelming majority occurring in August and September expect for once in 1961 that a little peak crossed the flood level during 10/7-10/10. Besides, linear regression suggests a strong correlation between basin-wide rainfall over upstream Ganges and river discharege at Hardinge Bridge.

3.1 Ganges basin and flood history

The drainage area of Ganges is 944,000 km^2 at Hardinge Bridge (Biancamaria et al, 2011). Webster et al. (2010) noted that flood level at Hardinge Bridge was 55,000 m^3/s. As the danger level at Hardinge Bridge is 14.25m (FFWC, 2007), a cross check between 55,000 m^3/s and 14.25m demonstrates that 55,000 m^3/s is effective as flood level at Hardinge Bridge. During 1951-2007 (the same period as precipitation records), water level at Hardinge Bridge exceeded the flood stage for 21

[3] It is short for Asian Precipitation-Highly-Resolved Observational Data Integration Towards Evaluation of Water Resources. This project has been conducted by the Research Institute for Humanity and Nature (RIHN) and the Meteorological Research Institute of Japan Meteorological Agency (MRI/JMA) since 2006. The detailed description is available online at http://www.chikyu.ac.jp/precip/.

years, with 1961, 1987, 1988 and 1998 encompassing both the highest peak and longest flood duration.

Table 1 displays the earliest and latest date that flood was on stage, the peak flow and flood duration time for each of the 21 flood years. It is clear that the earliest date flood started was August 14th, the latest date flood ended was October 10th, and it is still true when extending the period to all years with record (1934-2009). It is interesting to note that except for 1961 other years never experienced flood after end of September. To be more specific, flood happened during August and September for the overwhelming majority of years. For normal year, as peak could be considered to have the highest potential to develop into a flood, studying peak date would also provide useful clues. Table 2 lists the peak flow magnitude and date during normal years for the same period. It specifies that peak flow date in a normal year varies between 7/24 and 10/21, however, except for these two dates (for 2004 and 1985) other years all had peaks confined in August and September. Besides, Fig. 3 (left panel) shows how river discharge varies over the year in monthly scale. Both the tables and figure suggest that August-September is high-flow and highest-flood-risk period, and should be mainly focused on in flood forecasting.

Table 1Flood situation during 1951-2007

flood year	flood start date		flood end date		peak flow	duration (day)
	month	day	month	day		
1954	8	20	9	2	58600	13
1955	8	15	9	24	60300	21
1956	8	21	9	23	60100	14
1958	**8**	**14**	8	19	56300	6
1961	8	26	**10**	**10**	73200	28
1962	8	26	9	2	58700	8
1963	9	4	9	12	56100	6
1969	8	27	8	28	55200	2
1976	9	21	9	26	65400	6
1978	8	15	9	18	67900	18
1980	8	18	9	10	57800	13
1982	9	5	9	13	61600	9
1983	9	19	9	25	60000	7
1984	9	15	9	17	56500	3
1987	8	17	9	24	75800	25
1988	8	15	9	7	71800	24
1991	9	13	9	14	55600	2
1998	8	19	9	14	79059	27
1999	9	23	9	26	60292	4
2000	9	7	9	26	61445	18
2003	9	16	9	23	58481	8

*The earliest and latest flood dates are in red.

Table 2 Peak situation in normal years during 1951-2007

normal year	peak flow	peak flow date		normal year	peak flow	peak flow date	
		month	day			month	Day
1951	42200	8	30	1981	47900	8	30
1952	52600	9	5	1985	50300	**10**	**21**
1953	50900	8	29	1986	53500	8	28
1957	46200	9	10	1989	31500	9	8
1959	52700	8	19	1990	51000	8	21
1960	48000	9	4	1992	41800	9	21
1964	49000	9	11	1993	44700	9	22
1965	36800	9	16	1994	45900	8	18
1966	41900	9	1	1995	49100	9	15
1967	50800	9	17	1996	54062	9	5
1968	45200	8	29	1997	45031	9	7
1970	48700	9	23	2001	52311	8	31
1972	38200	9	8	2002	46055	8	1
1973	50700	9	20	2004	46808	**7**	**24**
1974	50700	9	2	2005	44309	9	2
1975	51100	8	30	2006	36941	8	31
1977	51100	8	14	2007	50677	8	6
1979	36900	8	2				

*The earliest and latest peak flow dates are in red.

Chowdhury and Ward (2004) noted that a peak is attained usually in late August or early September at Hardinge Bridge, and snowpack in the Himalayan tributaries have some impacts on it. It supports our argument that highest flood risk resides in Aug-Sep due to the peak time, and provides a clue that snowpack in the Himalayas might be somewhat responsible for the relative earlier or later arrival of flood/peak.

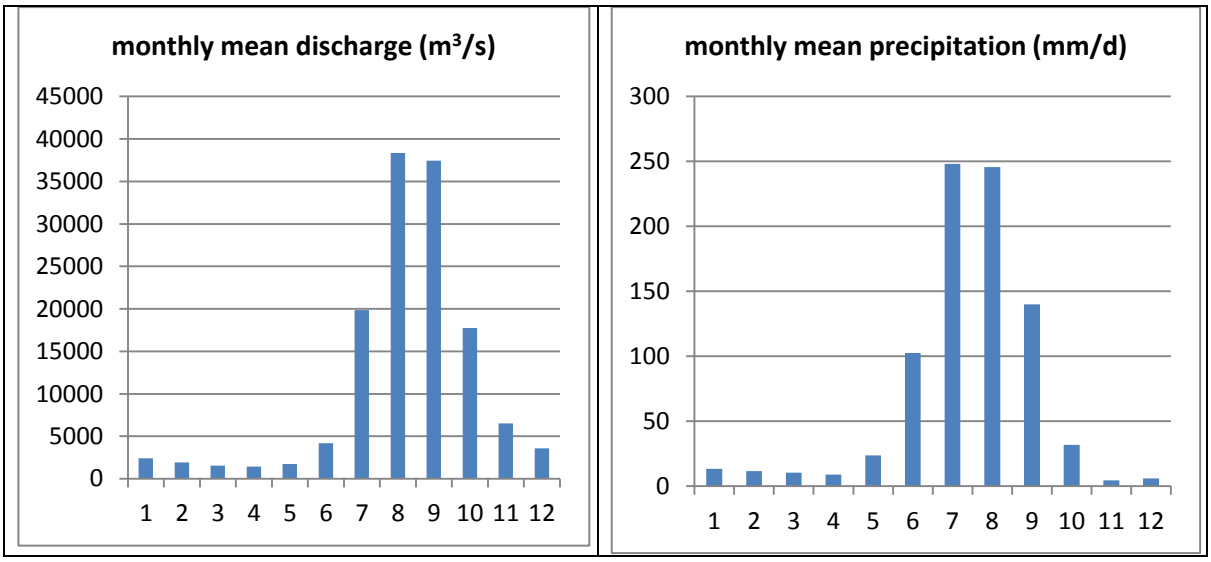

Figure 3 Monthly mean discharge at Hardinge Bridge and basin-average precipitation over Ganges basin

3.2 Temporal and spatial distribution of rainfall over Ganges basin

It takes rainfall different amount of time to travel from its original regions to Hardinge Bridge. To add appropriate lags to rainfall over Ganges basin, the Isochrones map for Ganges basin created by Webster et al. (2010) is used. The basin is divided into four rectangle domains (Fig.4). From west to east, they are named domain 1 to 4, whose size is 3°×4°, 3°×8°, 4°×7° and 4°×5°, and the water travel time range is 19-25, 13-18, 8-13 and 0-10 day, respectively.

Two types of average rainfall are calculated from the daily gridded data, one is domain-average rainfall, and the other is basin-average rainfall. Annual basin-average rainfall during 1951-2007 was

847 mm, with 87% of which received during the monsoon season from June to September, while July and August accounts for 29% of the annual rainfall each. Fig.3 (right panel) illustrates how basin-average rainfall distributes over the year in a monthly scale.

To examine the spatial rainfall variability, the four domain-average rainfall totals are compared to one other. The annual domain-average rainfall for domain 1 to 4 is 608, 845, 969 and 822 mm, respectively. Compared to annual basin-average rainfall 847 mm, domain 2 and 4 received normal range of rainfall, while domain 1 is deficient, and domain 3 is in excess.

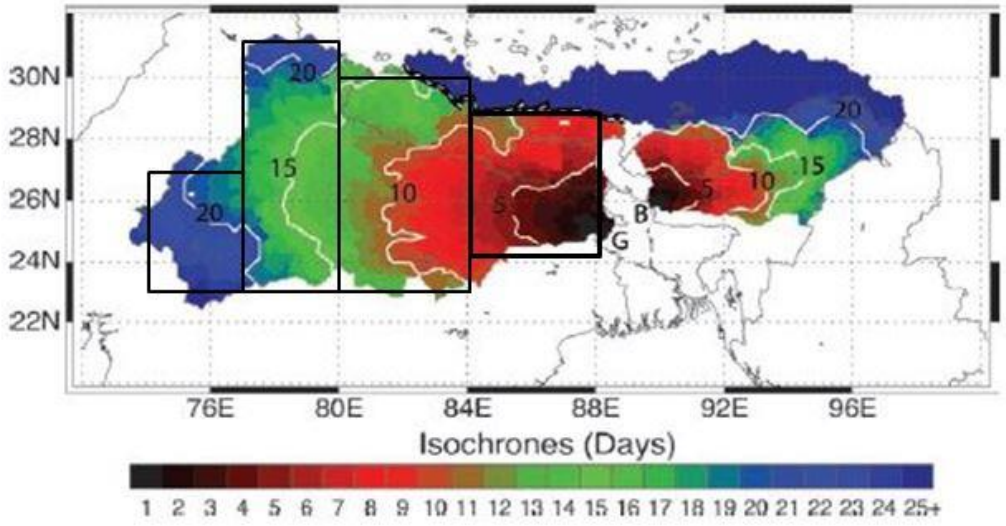

Figure 4 Travel-time-based domain division for Ganges basin.

The Isochrones were constructed by Webster et al. (2010) using flow routing algorithm and digital elevation data, the contours in Ganges basin (labeled as 'G') estimate the time (days) that water at a particular location needs to travel to Hardinge Bridge. The four black clear boxes roughly divide Ganges basin into four rectangle regions with different water travel time range.

3.3 Rainfall-Runoff relationship

It is interesting to note that the trend of monthly mean discharge at Hardinge Bridge is similar to that of basin-wide precipitation, with one-month lag in discharge (Fig. 3). However, the one-month doesn't have to be the actual lag, as it may decrease when finer time scale is used. And this should be true as Fig. 4 shows the longest water travel time is around 25 days, so the lag between rainfall and discharge would be smaller than that. Webster et al. (2010) plotted 10-d average basin-

wide precipitation over Ganges for 2004 (June-October), shifted it by 15-day forward, and found good relationship between it and daily discharge at Hardinge Bridge. Jian et al. (2009) made a similar plot for 1997, but shifted the rainfall by 13-day, and came to the same conclusion. There are more studies on their relationships, for example, Chowdhury and Ward (2004) found that the successive flows in July, August and September at Hardinge Bridge were highly correlated to rainfall received upstream over Ganges basin in June, July and August (r^2=0.54, 0.48, and 0.53), respectively; they also noticed that the seasonal flow (June-September, JJAS) was highly correlated to JJAS monsoon rainfall (r^2=0.565).

Based on the previously discussed findings, a linear regression between daily basin-average rainfall (with up to 24 lags) and daily river discharge was conducted. As discussed earlier, the highest flood risk occurs in August-September, it is more important to explore the correlation between rainfall and discharge during the two months. Fig. 3 suggests that during most of the year, rainfall is scarce and the flow is low, strengthening the annual relation between rainfall and river flow and providing a misleading measure of the predictability. Table 3 shows the correlation between basin-average precipitation P (with up to 24 lags) and river discharge at Hardinge Bridge Q for both whole-year and August-September. For whole-year, basin-average rainfall could explain 84% of variance in river discharge, however, for August-September only 37% of variance is explained. This speaks for the 'misleading measure of the predictability' mentioned earlier, as it is the 37% that matters in real flood forecasting practices instead of the 84%, and no one cares about low flow for the purpose of flood forecasting. Many researchers already realized this and reported results over the monsoon season (June-September) instead of the whole year. However, as flood risk is not equally distributed within the monsoon period but resides overwhelming concentrating in August-September, it makes sense to adjust the forecast system to focus on this period. The literature findings together with our preliminary results, demonstrates that upstream rainfall over Ganges basin has the potential to be a good predictor in flood forecasting.

Table 3 P—Q correlation (1951-2007)

P—Q	All-season	August-September
R^2 (pred)*	84%	37%

* R^2 (pred) is defined in equation (5).

4. A Simple Q—Q and Q+P—Q Model for Ganges

In this section, two statistical models are proposed to predict Ganges discharge at Hardinge Bridge, and comparisons are made among different lead-time. One is Q—Q model, where 'Q' denotes river discharge at Hardinge Bridge, the other is Q+P—Q model, where 'P' denotes upstream Ganges basin rainfall and more specifically the domain-average rainfall. Both models utilize flow persistence, and the difference is that Q+P—Q model also takes rainfall into account. To incorporate rainfall spatial variability, domain-average rainfall is used instead of basin-average rainfall. After introducing lagged domain-average rainfall, model performance improves compared to Q—Q model for all lead-time, especially beyond 5-day, thus making Q+P—Q model attractive for medium-range forecast. 'Perfect rainfall forecast', which provides rainfall forecast from the same data source as the previous rainfall, is also integrated into Q+P—Q model to evaluate potential model improvement when more accurate rainfall forecast becomes available in the future. Experiments suggest that for 10-day lead-time flood forecast, there exists an upper limit in model performance even with 'perfect rainfall forecast', and 6-day rainfall forecast is adequate for 10-day lead-time flood forecast. Flow records and rainfall data are both available during 1951-2007 (except 1971.4-1972.3), then it is divided into calibration (1951-1990) and validation (1991-2007) period.

4.1 A Persistence based Q—Q model

It is not unusual to rely on persistence to make predictions. Rahman et al. (2004) developed a simple approach for flood forecasting on Ganges at Hardinge Bridge, they divided each month during June-December into three 10-day periods, and then utilized the 10-day average flow to predict the average flow during other periods. They found most of the time, the best prediction (least errors between predicted and observed) occurred when using the adjacent period. The basis of their approach is flow persistence, and the smaller the lead-time, usually the better the prediction. Akhtar et al. (2009) concluded that at Hardinge Bridge, the previous flow had similar prediction ability in flow

forecasting within 7-day horizon compared to the previous flow plus rainfall options. Even the satellite altimetry technique used in water elevation forecasting at Hardinge Bridge (Biancamaria et al. 2011), utilized flow persistence. They found that the translation from upstream to downstream was mainly influenced by channel processes, and concluded that the highest accuracy occurred when lead-time equals flow travel time from 'virtual station' to Hardinge Bridge. Therefore, it is necessary to examine the flow persistence at Hardinge Bridge.

River discharge at Hardinge Bridge shows high persistence. For August and September, the autocorrelation function (ACF) of the dicharge is 0.98, 0.93, 0.75 and 0.48 for lag of 1, 2, 5 and 10 days, respectively. ACF reflects the correlation of time series data with itself, autocorrelation between times t and s is computed as follows:

$$ACF(s,t) = \frac{E[(X_t - \mu_t)(X_s - \mu_s)]}{\sigma_t \sigma_s} \quad (1)$$

where E is expectation operator, X_t and X_s are time series data at t and s, μ_t and μ_s are mean value of X_t and X_s, σ_t and σ_s are standard deviation of X_t and X_s. Therefore, Q—Q model is proposed, where Q denotes river flow, flow variables are introduced when noticeable improvement is added. Experiments suggest that current flow and the previous-day flow could represent the persistence forecast potential, and the model structure is as follows:

$$Q_{t+n} = \alpha Q_t + \beta Q_{t-1} + \gamma \quad (2)$$

where Q_{t+n} is river discharge at Hardinge Bridge on day (t+n), Q_t is river discharge on current day t, Q_{t-1} is river discharge on day (t-1), α, β and γ are model coefficients which are obtained from the calibration period. Forecasts are made on current day t.

Adjusted R^2 and root mean square error (RMSE) are defined as follows, and their values for different lead-time during validation period are shown in Table 4.

$$R^2 = 1 - \frac{\sum_{i=1}^{n}(y_i - \hat{y}_i)^2}{\sum_{i=1}^{n}(y_i - \bar{y})^2} \quad (3)$$

$$R^2(adj) = 1 - (1 - R^2)\frac{n-1}{n-p-1} \quad (4)$$

$$RMSE = \frac{1}{n}\sum_{i=1}^{n}(y_i - \hat{y}_i)^2 \quad (5)$$

where R^2 is coefficient of determination measuring how well the model fits the data, $R^2(adj)$ is adjusted R^2 taking the number of predictors into account, y_i is observation, $\hat{y}_i$ is the model estimate of y_i, $\bar{y}$ is average value of y_i, n is the number of observations, p is the number of non-constant predictors, and RMSE is root mean square error of the model.

The model performance is quite satisfying within 3-day lead-time, but R^2 (adj) decreases quickly from 91% to 74% when lead-time increases from 3-day to 5-day.

Table 4 Model performance for Aug/Sep flow of validation period (1991-2007)

Model	Q—Q				
Target	Q_{t+1}*	Q_{t+2}*	Q_{t+3}*	Q_{t+4}*	Q_{t+5}*
R^2(adj)	99%	96%	91%	83%	74%
RMSE	992	2197	3481	4725	5872

*day (t+n) is within August-September.

4.2 A simple Q+P—Q model

Rainfall is the major source of river flow in Ganges, other sources like snowmelt from Himalayas is not considered in the study as snow data is away from adequate. Groundwater outflow is not included, as in flood season the upstream heavy precipitation dominates the flow in the channel at Hardinge Bridge. Water loss (infiltration, evapotranspiration) and water diversion along Ganges are not taken into account either. But when fitting the model, as previous flow is input, snowmelt received at Hardinge Bridge on day t+n can be considered equal to that on day t; as domain-average rainfall is assigned different coefficients, the water loss rate can be assumed automatically proportional to the rainfall amount, which takes some water loss into consideration. However, for water diversions along Ganges, Hirpa et al. (2013) addressed that it was primarily designed for dry season but not during monsoon flood season, and the major diversions were assumed not to affect

Ganges discharge into Bangladesh beyond June 15. Therefore, it makes sense to omit the water diversion term. Though this model is simple, the coefficients for different domain-average rainfall variables allow for different level of rainfall-streamflow converting process for the four domains. Detailed and sophisticated hydrologic models are able to illustrate complicated physical process, but the added complexity introduces additional uncertainty and complicates any estimation of the uncertainty. This simple model, if demonstrated effective, may provide new dimensions in future water practices.

As discussed earlier, upstream rainfall has the potential to be a good predictor for flow at Hardinge Bridge and it is also the major drive in triggering flood, as a result, Q+P—Q model is proposed. Q denotes river flow at Hardinge Bridge, and P denotes upstream Ganges rainfall. The calculation of the domain-average rainfall is described in section 3. Here, the corresponding lags are added to domain-average rainfall based on the travel time ranges and no rainfall forecast is incorporated. The model uses only previous rainfall. The model structure is as follows:

$$Q_{t+n} = aQ_t + bQ_{t-1} + cRF_1 + dRF_2 + eRF_3 + fRF_4 + g \quad (6)$$

where Q_{t+n}, Q_t and Q_{t-1} denote the same as equation (2); RF_1, RF_2, RF_3 and RF_4 are lagged domain-average rainfall for domain 1 to 4; a, b, c, d, e, f, g are model coefficients obtained from calibration period. Comparisons between performances of the two models for validation period are present in Table 5.

It is clear that, within 5-day lead-time, contribution from rainfall is quite limited, R^2 (adj) only increases from 74% to 78% for 5-d lead-time forecast; however, beyond this horizon, the model improvement becomes noticeable, with R^2 (adj) increasing from 33% to 53% for 10-d lead-time forecast. Similar conclusion could be drawn from the study of Akhtar et al. (2009), they applied Artificial Neural Network (ANN) models to flow forecasting at Hardinge Bridge, and demonstrated little added value in introducing rainfall as input until 7-d lead-time.

Table 5 Comparisons of two models for validation period (1991-2007)

Model	target	R^2 (adj)	RMSE	Model	target	R^2 (adj)	RMSE
Q—Q	Q_{t+1}	99%	992	Q+P—Q	Q_{t+1}	99%	985
	Q_{t+2}	96%	2197		Q_{t+2}	97%	2157
	Q_{t+3}	91%	3481		Q_{t+3}	91%	3376
	Q_{t+4}	83%	4725		Q_{t+4}	85%	4494
	Q_{t+5}	74%	5872		Q_{t+5}	78%	5425
	Q_{t+6}	65%	6877		Q_{t+6}	72%	6138
	Q_{t+7}	55%	7736		Q_{t+7}	67%	6662
	Q_{t+8}	47%	8413		Q_{t+8}	63%	7035
	Q_{t+9}	39%	8989		Q_{t+9}	58%	7505
	Q_{t+10}	33%	9439		Q_{t+10}	53%	7939

Though the improvement beyond 5-day horizon is pronounced, the R^2 (adj) drops to 53% for 10-day lead-time, which is considered low. However, model performance is expected to improve when rainfall forecast is introduced.

4.3 Adding the 'perfect rainfall forecast'

Almost all flood forecast models utilize precipitation forecasts, even for hindcasts. There are several reasons for that, the precipitation data may not be available over the study area, or the time or spatial resolution of the data is not adequate due to the model setup. Rainfall re-analysis is quite popular in flood forecasting practices, for example ECMWF re-analysis (ERA-40) (Uppala et al., 2005) and the National Centers for Environmental Prediction/National Center for Atmospheric Research (NCEP/NCAR) re-analysis (Kalnay et al., 1996).

In this study, 'perfect rainfall forecast' is used instead of precipitation reanalysis, here the data is from the same source (APHRODITE) as previous studies, derived from rain-gauge-observation network. It is named as 'perfect rainfall forecast' because it actually represents the reality and couldn't be defeated by any forecast. It is widely accepted that inaccurate rainfall forecast is a major constraint in flow forecasting, however, in this case we demonstrate that there exists an upper limit even when 'perfect rainfall forecast' is available. The limitation comes from the unpredictable complexity in rainfall-runoff converting process and unreleased upstream information. For a basin

whose area is nearly 1,000,000 km^2, the restriction is even more rigorous. Table 6 displays model performance for 10-d lead-time flow forecasting when 'perfect rainfall forecast' lead-time varies from 0 to 10 days.

Table 6 Model results for different rainfall lead-time of validation period (1991-2007)

Model	target	Rainfall forecast lead-time (d)	R^2 (adj)	RMSE
Q+P—Q	Q_{t+10}	0	53%	7939
		1	57%	7576
		2	61%	7200
		3	64%	6968
		4	66%	6724
		5	68%	6515
		6	70%	6368
		7	70%	6292
		8	71%	6272
		9	70%	6305
		10	69%	6380

The improvement from 0 to 10-day rainfall forecast in flow prediction capability is expected. The highest predicting capability occurs with 8-day rainfall forecast. However, when rainfall forecast lead-time increases from 0 to 6 days, R^2 (adj) increases from 53 to 70%, and model performance is steady after that. It implies that with current methodology, 6-day rainfall forecast is adequate for 10-day lead-time flow forecast at Hardinge Bridge. The results demonstrate that if a short-range rainfall forecast is able to generate comparable flow forecast, then it's unnecessary to use extended rainfall forecasts to achieve better flow forecast. This is a powerful result given the limitations in long-range quantitative precipitation forecasts.

Fig. 5 shows plots comparing 10-day lead-time forecasted discharge with observed discharge for 1954 and 1998. These two years are selected to display because 1954 is a normal flood year while 1998 is the worst flood year ever for the country. Fig. 5 provides a clue on how the model performs for a particular year. For a normal flood year (1954), the model generally captures the peak and also demonstrates the capability to forecast the rising and recession limbs of the peak; however, the model misses the peak in an extreme flood year (1998) and loses the capability to predict high flows during

extreme flood events. This is probably because long-term calibration tends to maximize the average model performance, thus generating unsatisfying result for extreme flood years.

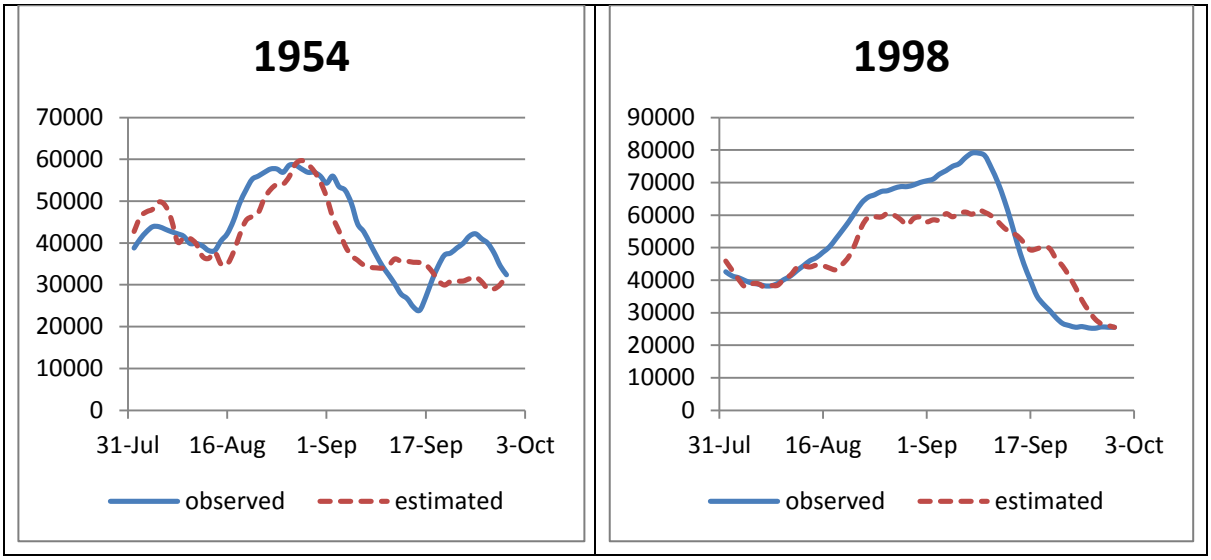

Figure 5 Forecasted discharge (10-day lead-time flood forecast with 6-day lead-time 'perfect rainfall forecast')

5. Impact of basin scale on forecasting ability: application of hybrid model

In this section, hybrid model (Nash and Barsi, 1983) is applied to Ganges flow forecasting, comparisons between performance of hybrid model and our proposed models are made. The proposed Q+P—Q model provides better performance than hybrid model for August-September flood forecasting. Two other rivers, Mississippi River at Clinton and Des Moines River at Keosauqua are selected to explore the impact of catchment scale on flow forecasting capability. The autocorrelation function of river discharge and Q—Q model results for the three rivers suggest that flow persistence and forecasting capability tend to decrease with basin scale.

Basin scale is a potential factor when researchers select the flow forecasting horizon, however, no paper has made specific statement on this issue yet, according to the author's knowledge. Komma et al. (2007) used 0-2-d forecast horizon for the 622 km^2 Kamp catchment in Austria. He et al. (2009) presented a case study on the 4062 km^2 catchment in England, and were able to provide 2.5-d lead-time in predicting the first peak and 4-d for the second peak during a flood event. Pappenberger et al. (2008) worked on Jiu River, one tributary on Danube in Romania, whose size is around 10,000 km^2. They reported that an efficient flood warning was issued at 5-d horizon and possible warning at 8-d. And for Ganges basin, whose drainage area is 944,000 km^2, Webster et al. (2010) reported forecast capability at 10-d horizon.

These examples imply that effective flow forecasting horizon and capability are very likely related to basin scale. It is also understandable, as small basins are highly sensitive to spatial and temporal precipitation pattern, large basins tend to smooth the effect of intense precipitation events. Consequently, for large basins, the basin-average precipitation is more important than the spatial and temporal pattern. Rainfall forecasting has long been the focus in improving flood forecasting capability, though a lot of efforts have been made, it hasn't been improved much since the past decades. However, it's not bad news for large catchments if the forecasting restriction from accurate

rainfall forecast becomes loose, and it may facilitate the establishment of a new scheme of flood forecasting for large-scale basins.

Alfieri et al. (2013) performed some meaningful work on this issue, they calculated Pearson correlation coefficient (PCC) of simulated versus observed discharge for 620 stations around the world, and plotted it against its upstream drainage area. They found a tendency of higher correlation in larger river basins, and the highest PCC values for the same upstream area generally increased with the upstream area. Their work laid a foundation for future research on impact of basin scale on flow forecasting ability.

To explore forecasting lead-time and ability for different basin sizes, another two rivers are studied, Mississippi River at Clinton and Des Moines River at Keosauqua. Their hydrographs are very different from Ganges (Fig. 6), the temporal variability in discharge is not as great as Ganges, and the high-flow months are also different. To make comparisons among their forecasting performances, the forecasting period is extended from August-September to whole-year. As the objective is to explore the impact of basin scale on forecasting performance instead of adding value to flood forecasting, the utilization of whole-year is reasonable. Different from section 4, there is no validation and the entire dataset is used for calibration.

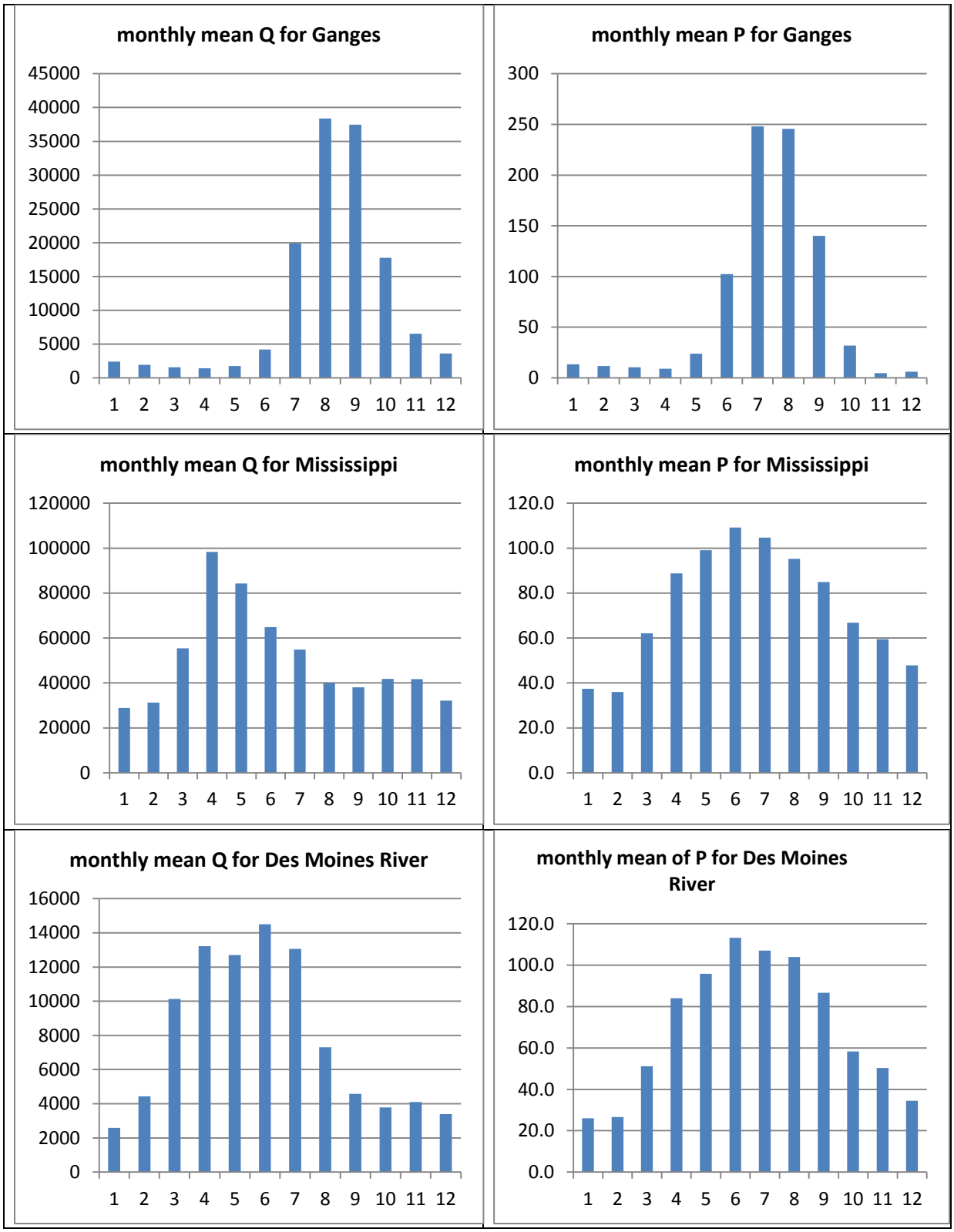

Figure 6 Monthly mean discharge and precipitation for three basins. 'Q' and 'P' denote discharge and basin-average precipitation.

Table 7 shows autocorrelation function (ACF) for three rivers. Compared to Ganges, ACF decreases more rapidly for Mississippi River at Clinton and Des Moines River at Keosauqua. It is not surprising, as flow persistence decreases with catchment size. As a result, Q—Q model performance deteriorates for smaller basins (Table 8). In Table 8, R^2 (pred) is predicted coefficient of determination representing the predicting ability of the present model. Each time one observation is removed, and assumed to be the prediction target, while the rest of data is used to obtain model coefficients. R^2 (pred) is computed as follows:

$$R^2(pred) = 1 - \frac{\sum_{j=1}^{n}(y_j - \widehat{y_j})^2}{\sum_{i=1}^{n}(y_i - \bar{y})^2} \quad (5)$$

Table 7 Autocorrelation function for three basins (whole-year)

Lag (d)	Ganges (944,000 km2)	Mississippi (221,703 km2)	Des Moines River (36,358 km2)
1	0.9979	0.9934	0.9713
2	0.9928	0.9789	0.9290
3	0.9852	0.9611	0.8961
4	0.9759	0.9417	0.8692
5	0.9657	0.9213	0.8453
6	0.9549	0.9000	0.8233
7	0.9440	0.8781	0.8020
8	0.9332	0.8558	0.7823
9	0.9224	0.8335	0.7653
10	0.9119	0.8113	0.7508
11	0.9014	0.7896	0.7376

5.1 Introduction to hybrid model

Nash and Barsi (1983) proposed a hybrid model for flow forecasting on large catchments, the hypothesis is that departures from seasonal mean for discharge and rainfall are linearly related, and basin-average rainfall is used in the model.

For Ganges, the seasonal mean explains 85% of variance in river discharge, while departures regression explains 42% of the remaining variance. And the basin-average rainfall departure of the

most recent 5 days (t, t-1… t-4) is not statistically significant in forecasting seasonal departure of discharge on day t, which automatically provides a 5-day lead-time for flow forecasting. In addition, as flow persistence has not been captured in hybrid model so far, and the residuals are found to contain some persistence structure that could be used. After residual updating procedure, 63% of the remaining variance is explained for 5-d lead-time forecast. Overall, for 5-d lead-time flow forecast at Hardinge Bridge, R^2 (pred) reaches 97% and root mean square error is 2620 using hybrid model, compared to 95% for R^2 (pred) and 3337 for RMSE using Q—Q model.

Table 8 Comparison of Q—Q model performances for three basins (whole-year)

Model	target	R-sq (pred)		
		Ganges (944,000 km2)	Mississippi (221,703 km2)	Des Moine River (36,358 km2)
Q—Q	Qt+1	100%	99%	95%
	Qt+2	99%	97%	86%
	Qt+3	98%	94%	80%
	Qt+4	97%	90%	76%
	Qt+5	95%	87%	71%
	Qt+6	93%	83%	68%
	Qt+7	91%	79%	64%
	Qt+8	89%	75%	61%
	Qt+9	87%	72%	59%
	Qt+10	85%	68%	56%

5.2 Comparisons of model performance between Q+P—Q model and hybrid model

10-day lead-time flow forecasting for Ganges is selected to compare hybrid model with the proposed Q+P—Q model, as it is a typical medium-range horizon and practically meaningful to prevent property loss and reduce agriculture costs.

For Aug/Sep flow forecasting, experiments suggest that the proposed Q+P—Q model provides better performance than hybrid model (Table 9). The utility of rainfall forecast is also assessed at 0, 5, 10-d ‘perfect rainfall forecast’. Similar conclusion could be drawn from hybrid model results, that it

doesn't noticeably decrease the model performance by leaving out rainfall of a few most recent days. This is consistent with previous model results (Table 6), and it is probably true that the most recent rainfall of a few days over Ganges basin won't noticeably influence the river discharge at Hardinge Bridge.

Table 9 10-day lead-time flow forecasting results of different models for Aug/Sep on Ganges

	Hybrid model		Q+P—Q	
	R^2 (pred)	RMSE	R^2 (pred)	RMSE
no rainfall forecast	51%	8019	53%	7939
5-day 'perfect rainfall forecast'	61%	7104	68%	6515
10-day 'perfect rainfall forecast'	62%	7057	69%	6380

5.3 Comparisons of model performances among three basins

As Nash and Barsi (1983) noted that their proposed hybrid model was expected to outperform many sophisticated models for highly seasonal catchments. Hybrid model is applied to the other two rivers and results for selected lead-time forecasting are shown in Table 10. Compared to Q—Q model in Table 8, hybrid model only shows advantage for Ganges, but provides similar performance as Q—Q model for both Mississippi and Des Moines River. It is probably because the two rivers hardly meet the "highly seasonal" requirement. Therefore, Q—Q model performance is used to measure the basin scale's impact on flow forecasting capability. As discussed earlier, Q—Q model becomes less efficient for smaller basins (Table 8). Table 8 also implies that forecasting ability and horizon deteriorate with catchment size.

Table 10 Hybrid model results for 5-day and 10-day lead-time forecast (whole year)

		Ganges (944,000 km^2)	Mississippi (221,703 km^2)	Des Moines River (36,358 km^2)
5-day (no RF forecast)	R-sq (pred)	97%	85%	70%
	RMSE	2,620	13,407	5,370
10-day (no RF forecast)	R-sq (pred)	92%	68%	54%
	RMSE	4,150	19,601	6,663
10-day (5-d RF forecast)	R-sq (pred)	94%	71%	59%
	RMSE	3,706	18,670	6,388
mean (m^3/s)		11,469	50,911	7,440
standard deviation (m^3/s)		14,773	34,177	9,158

6. Results and Discussion

6.1 Comparing Q—Q and Q+P—Q model

As suggested by Table 5, Q—Q model has comparable forecasting ability to Q+P—Q model within 5-day horizon. For 5-day lead-time forecast, adjusted R^2 is 74 and 78%, root mean square error (RMSE) is 5872 and 5425 for Q—Q and Q+P—Q model, respectively. And this conclusion is consistent with the result of Akhtar et al. (2009), that correlation coefficient is 0.866 and 0.87, RMSE is 5375 and 5290 for option 'Only Q' and 'TRF+Q'(Q is flow, TRF is sum of lagged rainfall, option 'TRF+Q' provides the best model performance among options containing rainfall within 5-day horizon), respectively. As they applied artificial neural network (ANN) models, the model structure is unknown. Only in a simple linear regression, the squared correlation coefficient equals R^2, so the results couldn't be compared in this metric. But both models use RMSE, and ANN model provides slightly lower RMSE. However, considering that the study period is quite different, they only use a few years' data, hence the results of the proposed models for 5-day forecast are viewed as comparable to their results.

One different conclusion drawn from two studies is the horizon when rainfall starts to add value. Akhtar et al. (2009) reported 7-day was the turning point, while 5-day is the case in this study. This may imply that the proposed approach to process rainfall in this study is more effective, as it is able to recognize rainfall contribution earlier. However, it can only demonstrate the advantage of domain-average rainfall over sum of rainfall, but inadequate for the comparison with 25 areal rainfall variables, as they only compared option 'Only Q' and 'TRF+Q', but discarded other options beyond 5-day horizon.

The reason why the inclusion of rainfall hardly improves the model performance within 5-day horizon, is that current and previous flow already contain much information and are dominant in determining the future flow. It suggests that for such a large basin, flow persistence is adequate in forecasting within 5-day horizon.

6.2 The utility of rainfall forecast

Table 6 presents model results of 10-day lead-time forecast, which incorporates rainfall forecast with different lead-time. It is clear that highest adjusted R^2 and lowest RMSE are obtained when rainfall forecast lead-time is 8-day. Compared to flow forecast with no rainfall forecast, it increases R^2 (adj) from 53 to 71%, and decreases RMSE from 7939 to 6272. Looking closely, results show a relatively steady trend after 6-day rainfall forecast. As the model improvement in flood forecast from 6-day to 8-day rainfall forecast is considered minor, which is 1% increase in R^2 (adj) and less than 100 (m^3/s) decrease in RMSE, 6-day rainfall forecast is viewed to have comparable forecasting potential for 10-day lead-time.

The fact that for 10-day lead-time flow forecast, the best prediction ability doesn't occur when using 10-day rainfall forecast, indicates that with current methodology, it's unnecessary to use rainfall during the most recent 2-day, and the result won't change much if the most recent 4-day rainfall is left out. It is not surprising, as the average water travel time in domain 4 (the nearest domain to Hardinge Bridge) is 5 days. When it comes to domain-average rainfall, ideally domain 4 is viewed as a point, and rainfall falling over domain 4 at present day t arrives at Hardinge Bridge at day t+5 on average, therefore, the most recent 4-day's rainfall won't matter much.

Given the limitations in long-range quantitative precipitation forecasts, it is a powerful result that full-range rainfall forecast (where rainfall forecast lead-time matches with flood forecast lead-time) is unnecessary. However, this depends on both the basin scale and the proposed methodology.

6.3 The impact of basin scale on forecasting ability

It is common that researchers consider basin scale when selecting flow forecast horizon, long-range forecast is possible for large basins while only short-range forecast is considered for small basins. It is easy to understand, and there are two aspects, first is flow persistence increases with basin scale, second is the impact of rainfall temporal and spatial variability on forecasting decreases with basin scale. Table 8 shows the predicted R^2 decreases with basin scale for Q—Q model, thus proving flow persistence decreases with basin scale. The second aspect hasn't been assessed in this thesis, and can be studied in future work.

There are several challenges for this issue. First, the forecasting ability needs to be specified, not only the measures but also the lead-time. Pearson correlation coefficient (PCC) between forecasted and observed values is a good indicator, but the forecast horizon cannot be ignored either. To unify these two perspectives, a threshold for PCC can be established, value higher than it can be considered as acceptable, and then the lead-time could be analyzed against the basin scale. Second, theoretically a general approach/model needs to be applied for different basins, however, it might be unfair for some basins, as basins benefit differently from the same model. Hence, modifications or adjustments need to be made for different basins, which may lead to large amount of work. Of course, the present results in literatures are available to use, but they usually study different length of period and report different metrics in evaluating their model performance, making it difficult to compare their results.

7. APPENDIX

In earlier stage of this research, large amount of work has been done on rainfall over domain 4 (the closest domain to Hardinge Bridge) to try to distinguish flood from non-flood years. These findings are not shown in this thesis, but attached as appendix here.

Every year right before flood happened, or before peak flow for non-flood years, a window of n-day period is studied. Initial hypothesis proposed is that flood is caused by a series of storm events instead of single event, this is why a n-day window is studied instead of single precipitation event. Analyses using both NCEP-NCAR re-analysis and APHRODITE are both shown on exploring the n-day period before flood/peak to distinguish them. Both suggest that the 14-day period before flood/peak is the most effective 'cutoff'. The accumulative rainfall as well as the daily rainfall during 14-day period is studied and compared between flood and non-flood years. Result suggests that the accumulative rainfall during the period can separate 71% of flood years from 63% of non-flood years, and the inclusion of daily rainfall pattern fails to improve the separation.

A build-up analysis on accumulative rainfall during monsoon season before flood/peak and accumulative rainfall during June-July is also conducted, but minor difference occurs between flood and non-flood years. However, the comparison in monthly rainfall suggests that the biggest difference between flood and non-flood years occurs in August. To further explores the potential contribution of August rainfall to the separation, daily average rainfall is calculated during August 1 to flood/peak, and the result suggests that the daily average rainfall of 6.2 mm can separate 81% of flood years from 70% of non-flood years, which is the best result from the analyses on rainfall over domain 4.

Summary of NCEP-NCAR data analysis

(NCEP/NCAR re-analysis data is used for rainfall over domain 4)

Table 1 n-day total amount of rainfall before flood/peak

	"cutoff"(mm)	flood year	non-flood year
10-day	93-100	9/22 exceeds	34/38 below
11-day	101-109	10/22 exceeds	33/38 below
12-day	"cutoff" line not meaningful		
13-day	"cutoff" line not meaningful		
14-day	122-125	16/22 exceeds	27/38 below
15-day	134	16/22 exceeds	28/38 below
16-day	141-144	16/22 exceeds	28/38 below
17-day	150-153	16/22 exceeds	28/38 below
18-day	158-159	16/22 exceeds	28/38 below
19-day	168-174	16/22 exceeds	29/38 below
20-day	179-182	16/22 exceeds	30/38 below
21-day	187-190	16/22 exceeds	30/38 below
22-day	198-199	16/22 exceeds	29/38 below
23-day	200-206	16/22 exceeds	28/38 below
24-day	211-214	16/22 exceeds	28/38 below
25-day	215-217	17/22 exceeds	26/38 below
26-day	230	16/22 exceeds	29/38 below
27-day	238	17/22 exceeds	29/38 below
28-day	248-249	16/22 exceeds	29/38 below
29-day	257	16/22 exceeds	28/38 below
30-day	266-267	16/22 exceeds	28/38 below

*The goal of "cutoff" is to separate flood years from non-flood years,
as it is impossible to make 100% separation, the more separated, the better.

In Table 1, after 14-day totals the effectiveness of "cutoff" line is relatively steady. Figure 1 shows strong linear correlation between average 'cutoff' line and number of days, this may implies that the slope is the minimum requirement of daily rainfall in leading to floods.

Next daily rainfall distribution within the 14-day period is studied.

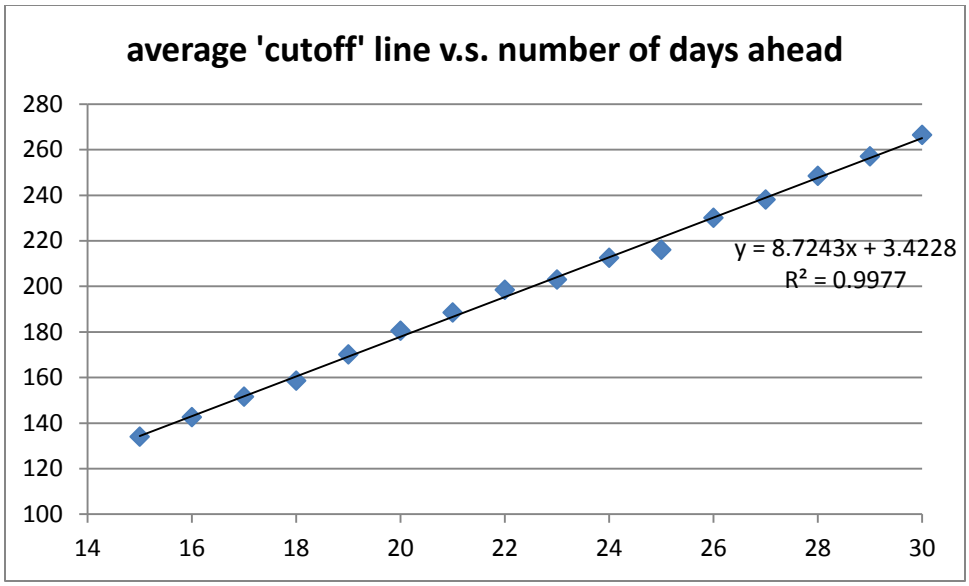

Figure 1 Average 'cutoff' line vs number of days (NECP/NCAR)

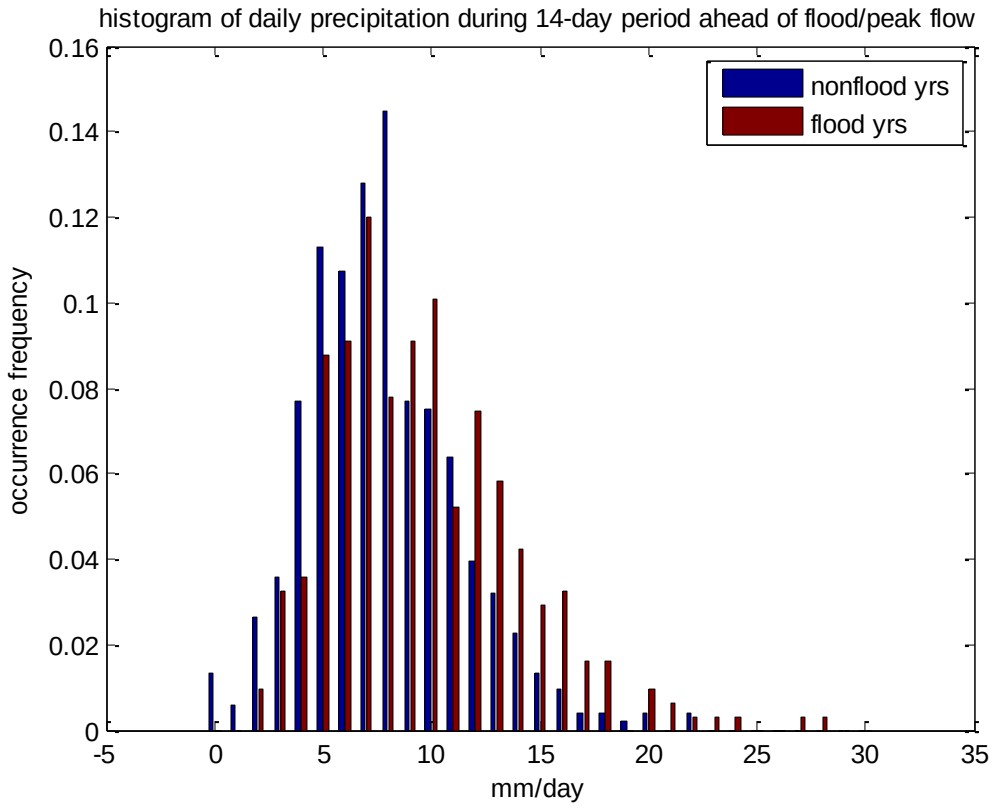

Figure 2

Figure 2 shows daily rainfall distribution during 14-day period, which is what we identified as contributing period to flood events. Flood years (red bars) show a shift to right compared with non-flood years (blue bars). Statistical results are listed as following (unit: mm):

Flood years: mean=9.6, standard deviation=4.4;

Non-flood years: mean=7.8, standard deviation=3.5.

It is noticeable that flood years exceed non-flood years after 8mm in bars, which means if there is a day (during 14-day period)with smaller than 9mm of rainfall, whatever the exact amount is, we can say that it has higher chance to be in non-flood years than flood years, according to Figure 2. Otherwise, if that day exceeds 9mm rainfall, except for 11mm and 22mm (blue bars higher than red), we can say this day has higher probability to be in flood years.

If we draw cdf figure, we will get a better idea of how different they are.

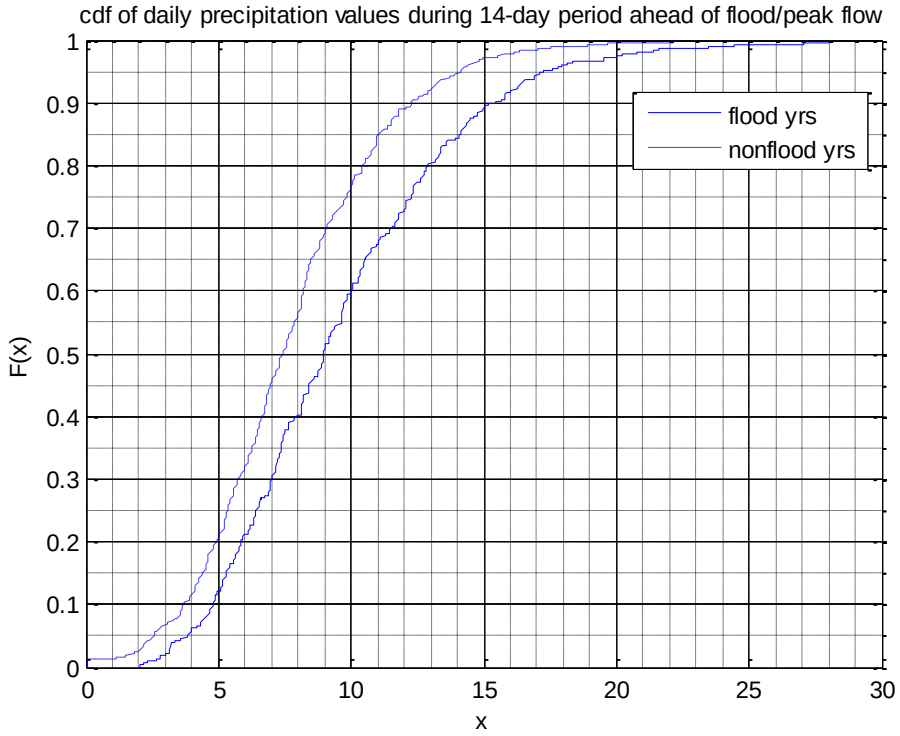

Figure 3

From Figure 3, the biggest distinction occurs at x=9mm/day, consistent with Figure 2. Take 9mm/day as example, 50% of days during 14-day period in flood years exceeds this daily value; while only 30% of days during 14-day period in non-flood years exceeds. Therefore, if a specific day's (in 14-day period) rainfall exceeds 9mm, its probability to be in flood year is 50/(50+30)=62.5%, while its chance to be in non-flood year is 30/(50+30)=37.5%.

Now we get a clue that 9mm/day might be a 'threshold' between flood/non-flood years. Back to our original hypothesis, a sequence of storms instead of single extreme storm may lead to flood. Next we will see how number of storm days plays a role in distinguishing flood and non-flood years. However, as precipitation is extremely frequent, almost every day during 14-day period, I use 9mm as a 'threshold' to consider rainfall as effective storm to contribute to flood.

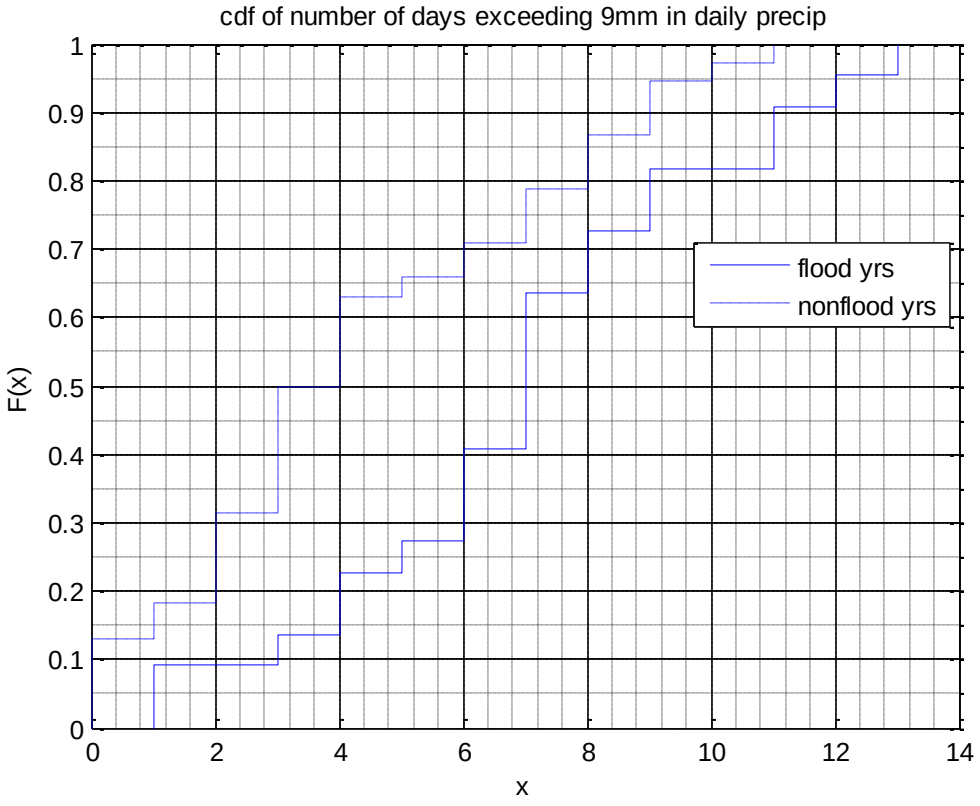

Figure 4

Figure 4 is empirical cdf for number of days exceeding 9mm of daily rainfall during the 14-day period. The biggest jump occurs at 5 days, which means 5 days of greater than 9mm daily rainfall during 14-day period is the most probable distinction between flood/non-flood years. There are 77% of flood years which have greater than 5 (or at least 6) days exceeding 9mm of daily rainfall during 14-day period, while only 37% of non-flood years do. Therefore, during 14-day period, if we have >5 days of >9mm of daily rainfall, the chance of being in a flood year is 77/(77+37)=67.5%, while chance for non-flood year is 37/(77+37)=32.5%; that is to say, if we get at least 6 days of >9mm daily rainfall before, the chance of leading to a flood is 67.5%.

Summary of Aphrodite data analysis

Table 2 'cutoff' line for n-day totals (Aphrodite data)

n-day period	cutoff (mm)	average cutoff	exceedance percentage	
			flood year	non-flood year
8	67	67	48%	14%
9	82	82	43%	9%
10	78-79	78.5	57%	29%
11	79-80	79.5	71%	43%
12	85	85	71%	43%
13	91-92	91.5	67%	37%
14	**94-95**	**94.5**	**71%**	**37%**
15	99-101	100	67%	37%
16	98	98	81%	51%
17	125-127	126	53%	23%
18	129-132	130.5	57%	23%
19	135-139	137	57%	23%
20	145	145	57%	17%
21	152-156	154	52%	17%
22	159-164	161.5	53%	17%
23	166-167	166.5	57%	20%
24	178	178	52%	14%
25	181-182	181.5	52%	17%
26	187-188	187.5	52%	17%
27	186-188	187	62%	26%
28	199	199	62%	20%
29	204	204	62%	20%
30	210-213	211.5	62%	20%

Table 2 suggests '14-day totals' is the most effective 'cutoff' line, which is consistent with Table 1. As they are results from different data sources, it is reliable to use '14-day totals' as an indicator to distinguish flood years from non-flood years. Here the '14-day totals' cutoff can separate 71% of flood years from 63% of non-flood years.

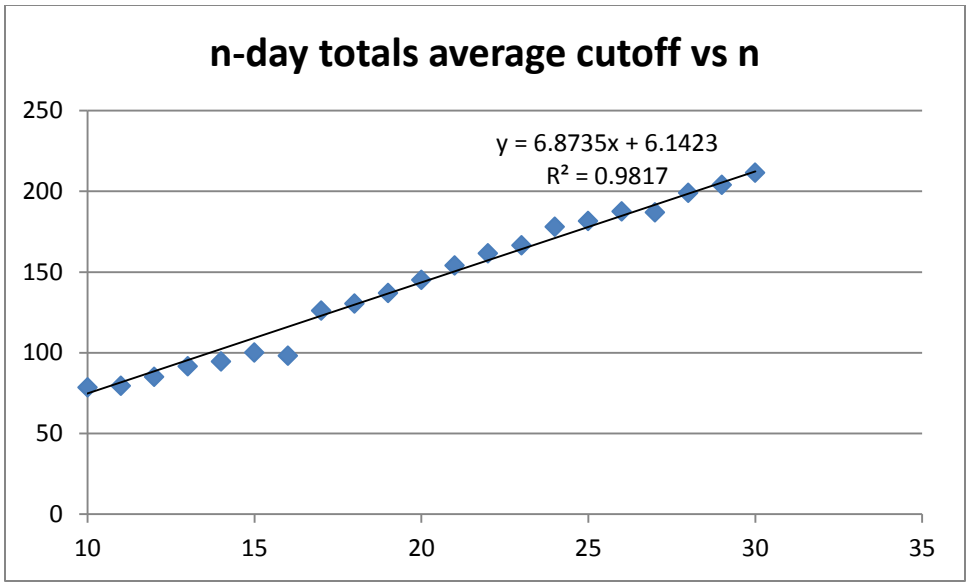

Figure 5 n-day totals average 'cutoff' line vs number of days

Figure 5 also shows a linear correlation between average 'cutoff' and number of days, but 16-day totals 'cutoff' behaves differently, it is even smaller than 15-day totals 'cutoff'. The reason is not explored here. Similarly, the slope seems to be the minimum requirement for daily rainfall to cause floods.

Next let's look at other indicators which might help to separate flood from non-flood years.

Daily rainfall pattern within the 14-day period

Similar to Figure 3, Figure 6 shows cdf of daily rainfall within the 14-day window before flood/peak for each year, and it suggests that the biggest difference occurs at 4mm. Similar to Figure 4, Figure 7 shows cdf of number of days exceeding 4mm during the period, and it suggests that the biggest difference occurs at 10 days. Combining these two requirements, another indicator to separate flood and non-flood years is proposed, which is during the 14-day window right before flood/peak, at least 11 days exceed 4mm in daily precipitation.

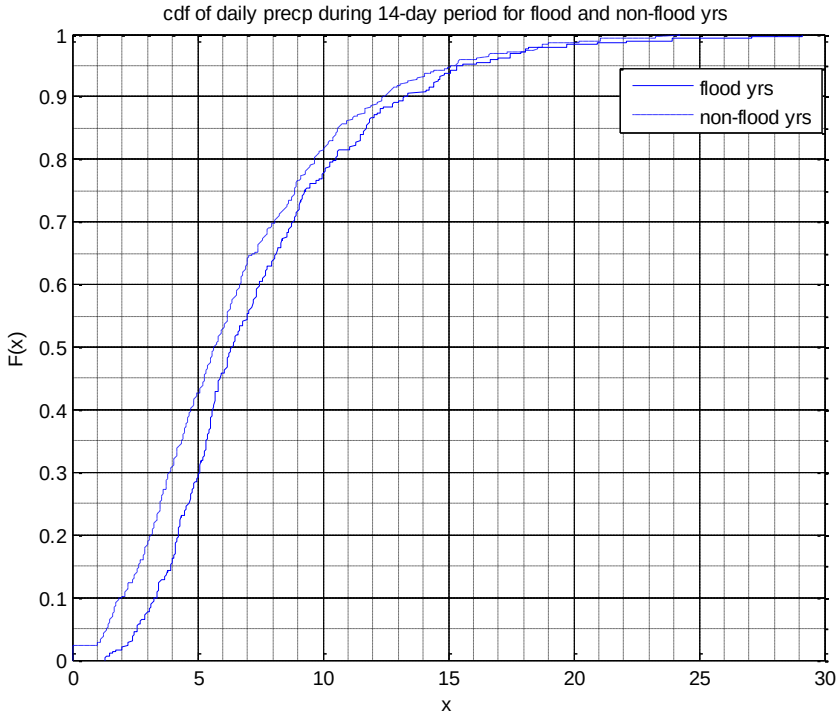

Figure 6

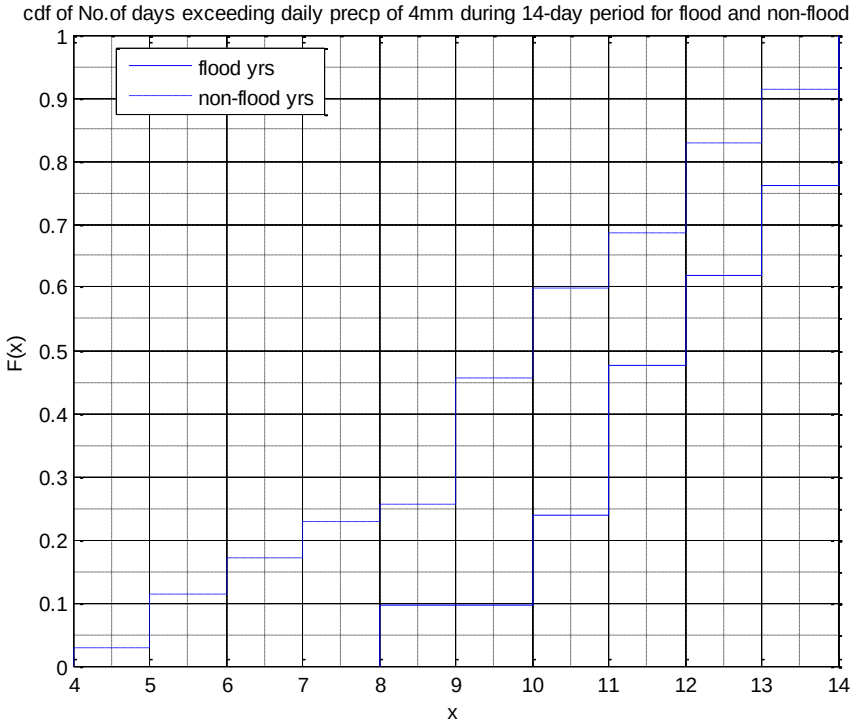

Figure 7

Build-up analysis

As runoff comes from excess rainfall which the soil couldn't absorb, it may provide some clue when exploring the total amount of rainfall before flood/peak. Table 3 suggests that there is no big difference in average accumulative rainfall before flood/peak between flood and non-flood years.

Table 3 Accumulative rainfall during June-flood/peak (unit: mm)

non-flood year	totals ahead	flood year	totals ahead
1951	517	1954	563
1952	588	1955	616
1953	624	1956	473
1957	556	1958	432
1959	416	1961	510
1960	558	1962	538
1964	620	1963	573
1965	582	1969	530
1966	490	1976	639
1967	541	1978	473
1968	586	1980	502
1970	683	1982	441
1972	470	1983	570
1973	645	1984	761
1974	633	1987	548
1975	515	1988	500
1977	440	1991	651
1979	349	1998	588
1981	538	1999	783
1985	814	2000	619
1986	476	2003	635
1989	546	average	569
1990	515		
1992	519		
1993	636		
1994	404		
1995	622		
1996	618		
1997	573		
2001	523		
2002	380		
2004	387		
2005	499		
2006	425		
2007	438		
average	535		

Table 4 shows June-July accumulative rainfall for all years, similarly difference between flood and non-flood years on average totals is minor.

Table 4 June-July accumulative rainfall for non-flood and flood years (unit: mm)

Non-flood years	June-July totals	flood years	June-July totals
1951	349	1954	432
1952	358	1955	506
1953	468	1956	370
1957	337	1958	257
1959	277	1961	319
1960	308	1962	316
1964	395	1963	360
1965	312	1969	338
1966	272	1976	319
1967	296	1978	375
1968	411	1980	373
1970	390	1982	296
1971	393	1983	309
1972	271	1984	483
1973	343	1987	357
1974	407	1988	379
1975	383	1991	320
1977	361	1998	407
1979	343	1999	441
1981	371	2000	375
1985	378	2003	397
1986	330	average	368
1989	363		
1990	400		
1992	274		
1993	309		
1994	292		
1995	360		
1996	370		
1997	358		
2001	354		
2002	380		
2004	428		
2005	291		
2006	292		
2007	416		
average	351		

The build-up analysis fails to provide useful indicator to separate flood from non-flood years. Now let's look at if it help the separation to combine '14-day totals' with '11 days of >4mm in daily rainfall' in the separation.

Table 5 Results from two combined 'cutoff'

Non-flood year	14-day totals	No of days>4mm	separated?	flood year	14-day totals	No of days>4mm	separated?
1951	111	10	1	1954	100	11	1
1952	111	11	0	1955	111	14	1
1953	105	9	1	1956	95	11	1
1957	77	9	1	1958	185	14	1
1959	109	12	0	1961	101	14	1
1960	151	14	0	1962	129	13	1
1964	88	9	1	1963	85	11	0
1965	47	5	1	1969	118	13	1
1966	110	13	0	1976	103	10	0
1967	55	6	1	1978	99	13	1
1968	91	12	1	1980	105	14	1
1970	87	11	1	1982	66	10	0
1972	76	9	1	1983	80	12	0
1973	92	11	1	1984	110	11	1
1974	110	12	0	1987	149	8	0
1975	71	10	1	1988	121	12	1
1977	88	12	1	1991	122	12	1
1979	140	14	0	1998	138	14	1
1981	93	9	1	1999	57	8	0
1985	85	6	1	2000	91	11	0
1986	93	10	1	2003	65	10	0
1989	60	5	1	failures			8
1990	86	8	1				
1992	48	4	1				
1993	59	7	1				
1994	101	10	1				
1995	54	5	1				
1996	77	9	1				
1997	67	7	1				
2001	106	14	0				
2002	142	13	0				
2004	122	13	0				
2005	91	9	1				
2006	80	10	1				
2007	158	12	0				
failures			10				

Table 5 displays the results, 62% (13/21) of flood years are separated from 71% (25/35) of non-flood years. Compared with the results from ’14-day totals’ from Table 2, which is 71% of flood years are separated from 63% of non-flood years, the performance only increases for non-flood years but decreases for flood years. Considering that it is more important to recognize flood years, the combined ‘cutoff’ is considered no better than ’14-day totals’ cutoff.

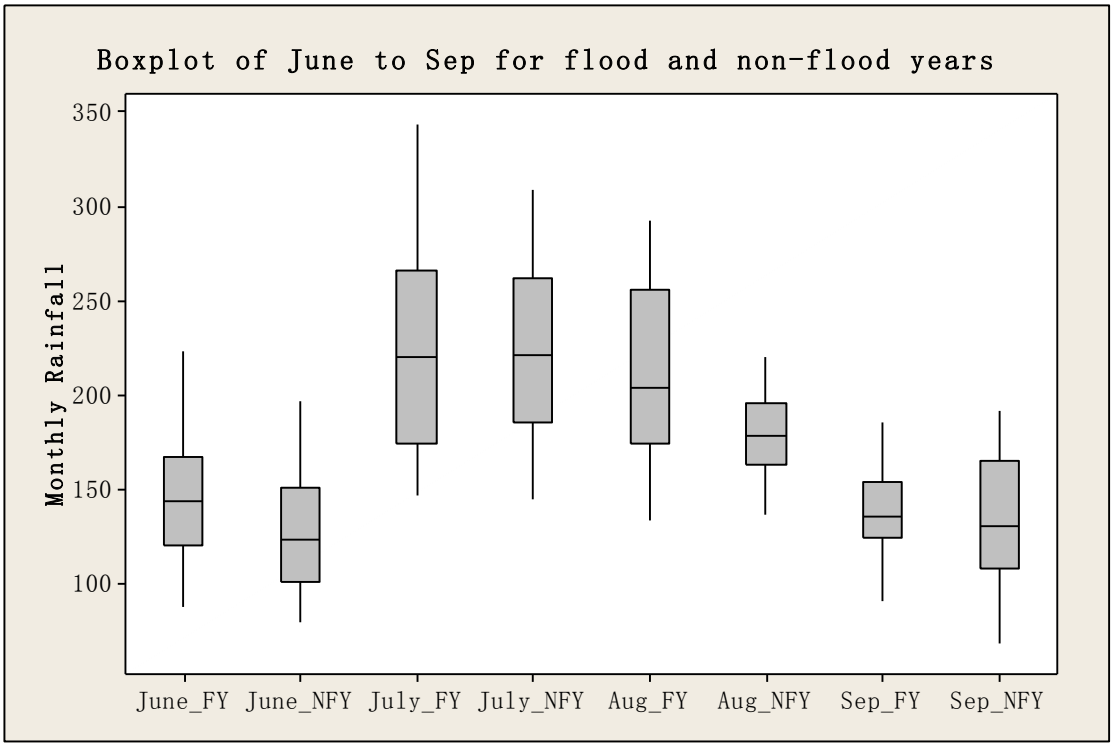

Figure 8 Boxplot of monthly rainfall in June to Sep for flood and non-flood years

Figure 8 shows the comparison of boxplot of monthly rainfall between flood and non-flood years, it implies a further study on August rainfall as the biggest difference occurs here. Therefore, daily average rainfall during Aug 1 to flood/peak is calculated for each year, as shown in Table 5. It suggests that 81% (17/21) of flood years have daily average rainfall greater than 6.2mm, while 70% (23/33) of non-flood years fall below 6.2mm. That is to say, over 80% of flood years can be separated from 70% of non-flood years using this daily average ‘cutoff’. This is very similar to the n-day period analysis as described earlier, the end date of the study period is fixed for both analyses, the start date is fixed here but the length

of period is fixed in previous analysis. However, this analysis gives better result than the previous one. And this is the best result obtained from all analyses on rainfall over domain 4.

Table 6 Daily average rainfall during August 1 to flood/peak

flood year		non-flood year	
1982	4.1	2007	4.5
2003	5.2	2006	4.5
1956	5.2	1975	4.6
1983	5.3	1992	4.8
1984	6.2	1989	4.8
1963	6.3	1967	5.2
1976	6.3	1972	5.2
1999	6.4	1985	5.4
2000	6.6	1986	5.4
1954	6.9	1979	5.4
1978	7.1	1957	5.5
1969	7.4	1964	5.5
1961	7.6	1970	5.5
1980	7.6	1953	5.6
1991	7.7	2001	5.7
1955	7.9	1981	5.7
1988	8.7	1990	5.8
1962	8.9	1951	5.8
1998	10.0	1997	5.8
1987	11.9	1995	5.8
1958	13.4	1965	5.9
		1973	6.0
		1977	6.1
		1968	6.3
		1993	6.3
		2005	6.5
		1994	6.6
		1952	6.6
		1966	7.0
		1974	7.1
		1996	7.1
		1960	7.4
		1959	7.7

8. REFERENCES

Akhtar, M. K., Corzo, G. A., Van Andel, S. J., & Jonoski, A. (2009). River flow forecasting with artificial neural networks using satellite observed precipitation pre-processed with flow length and travel time information: Case study of the ganges river basin. Hydrology and Earth System Sciences, 13(9), 1607-1618.

ADPC, 2002: Application of climate forecasts in the agriculture sector. Climate Forecasting Applications in Bangladesh Project Rep. 3, Asian Disaster Preparedness Center, Bangkok, Thailand, 29 pp.

Alfieri, L., Burek, P., Dutra, E., Krzeminski, B., Muraro, D., Thielen, J., & Pappenberger, F. (2013). GloFAS-global ensemble streamflow forecasting and flood early warning. Hydrology and Earth System Sciences, 17(3), 1161-1175.

Brammer, H. (1990). Floods in bangladesh: I. geographical background to the 1987 and 1988 floods. Geographical Journal, 156(1), 12-22.

Bindlish, R., Crow, W. T., & Jackson, T. J. (2009). Role of passive microwave remote sensing in improving flood forecasts. IEEE Geoscience and Remote Sensing Letters, 6(1), 112-116.

Cloke, H. L., & Pappenberger, F. (2009). Ensemble flood forecasting: A review. Journal of Hydrology, 375(3-4), 613-626.

CEGIS, 2006: Centre for Environmental and Geographical Service (CEGIS) Early Warning System. Final Rep. to the Asian Development bank, 263 pp. [Available online at http://cfan.eas.gatech.edu/PJWebster/Floods/.]

Chowdhury, M. R., & Ward, M. N. (2007). Seasonal flooding in bangladesh - variability and predictability. Hydrological Processes, 21(3), 335-347.

Chowdhury, M. R., & Ward, M. N. (2003). Seasonal rainfall and stream-flow in the ganges-brahmaputra basins of bangladesh: Variability and predictability. World Water and Environmental Resources Congress, 2549-2558.

Chowdhury, R., & Ward, N. (2004). Hydro-meteorological variability in the greater ganges-brahmaputra-meghna basins. International Journal of Climatology, 24(12), 1495-1508.

Dechant, C., & Moradkhani, H. (2011). Radiance data assimilation for operational snow and streamflow forecasting. Advances in Water Resources, 34(3), 351-364. doi:http://dx.doi.org/10.1016/j.advwatres.2010.12.009

FFWC: Flood Forecasting and Warning Center; Annual Flood Report 2007, Technical Rep., Dhaka, Bangladesh.

Hopson, T. M., & Webster, P. J. (2010). A 1-10-day ensemble forecasting scheme for the major river basins of bangladesh: Forecasting severe floods of 2003-07. Journal of Hydrometeorology, 11(3), 618-641.

Hossain, M., Islam, A. T. M. A . and Saha, S. K. 1987 Floods in Bangladesh: recurrent disaster and people's survival. Dhaka: Univ. Res. Centre.

He, Y., Wetterhall, F., Cloke, H. L., Pappenberger, F., Wilson, M., Freer, J., & McGregor, G. (2009). Tracking the uncertainty in flood alerts driven by grand ensemble weather predictions. Meteorological Applications, 16(1), 91-101.

Hirpa, F. A., Hopson, T. M., De Groeve, T., Brakenridge, G. R., Gebremichael, M., & Restrepo, P. J. (2013). Upstream satellite remote sensing for river discharge forecasting: Application to major rivers in south asia. Remote Sensing of Environment, 131, 140-151.

Jian, J., Webster, P. J., & Hoyos, C. D. (2009). Large-scale controls on ganges and brahmaputra river discharge on intraseasonal and seasonal times-cales. Quarterly Journal of the Royal Meteorological Society, 135(639), 353-370.

Jakobsen, F., Hoque, A. K. M. Z., Paudyal, G. N., & Bhuiyan, M. S. (2005). Evaluation of the short-term processes forcing the monsoon river floods in bangladesh. Water International, 30(3), 389-399.

Kalnay, E., Kanamitsu, M., Kistler, R., Collins, W., Deaven, D., Gandin, L., & Joseph, D. (1996). The NCEP/NCAR 40-year reanalysis project. Bull. Am. Meteorol Soc., 77, 437–471.

Komma, J., Reszler, C., Blöschl, G., & Haiden, T. (2007). Ensemble prediction of floods - catchment non-linearity and forecast probabilities. Natural Hazards and Earth System Science, 7(4), 1-14.

Monirul Qader Mirza, M., Warrick, R. A., Ericksen, N. J., & Kenny, G. J. (2001). Are floods getting worse in the ganges, brahmaputra and meghna basins? Environmental Hazards, 3(2), 37-48.

Mirza, M. M. Q. (2003). Three recent extreme floods in bangladesh: A hydro-meteorological analysis. Natural Hazards, 28(1), 35-64.

Montgomery, R. (1985). The bangladesh floods of 1984 in historical context (crop losses). Disasters, 9(3), 163-172.

Nash, J. E., & Barsi, B. I. (1983). A hybrid model for flow forecasting on large catchments. Journal of Hydrology, 65(1-3), 125-137.

Pappenberger, F., Bartholmes, J., Thielen, J., Cloke, H. L., Buizza, R., & de Roo, A. (2008). New dimensions in early flood warning across the globe using grand-ensemble weather predictions. Geophysical Research Letters, 35(10).

Paudyal, G. N. (2001). Forecasting and warning of water related disasters in a complex hydraulic setting - the case of bangladesh. Journal of Indian Water Works Association, 33(1), 75-79.

Rasid, H., & Paul, B. K. (1987). Flood problems in bangladesh: Is there an indigenous solution? Environmental Management, 11(2), 155-173.

Rahman, M., Khan, S. M., & Pasha, F. K. (2004). Simple approach for flood forecasting. Joint Conference on Water Resource Engineering and Water Resources Planning and Management 2000: Building Partnerships, 104.

Siddique-E-Akbor, A. H. M., Hossain, F., Lee, H., & Shum, C. K. (2011). Inter-comparison study of water level estimates derived from hydrodynamic–hydrologic model and satellite altimetry for a complex deltaic environment. Remote Sensing of Environment, 115(6), 1522-1531. doi:http://dx.doi.org/10.1016/j.rse.2011.02.011

Thielen, J., Bogner, K., Pappenberger, F., Kalas, M., del Medico, M., & de Roo, A. (2009). Monthly-, medium-, and short-range flood warning: Testing the limits of predictability. Meteorological Applications, 16(1), 77-90.

Uppala, S. M., Kållberg, P. W., Simmons, A. J., Andrae, U., da Costa Bechtold, V., Fiorino, M., . . . Woollen, J. (2005). The ERA-40 re-analysis. Quarterly Journal of the Royal Meteorological Society, 131(612), 2961-3012.

Vitart, F. (2004). Monthly forecasting at ECMWF. Monthly Weather Review, 132(12), 2761-2779.
Biancamaria, S., Hossain, F., & Lettenmaier, D. P. (2011). Forecasting transboundary river water elevations from space. Geophysical Research Letters, 38(11).

Webster, P. J., Jian, J., Hopson, T. M., Hoyos, C. D., Agudelo, P. A., Chang, H. -., . . . Subbiah, A. R. (2010). Extended-range probabilistic forecasts of ganges and brahmaputra floods in bangladesh. Bulletin of the American Meteorological Society, 91(11), 1493-1514.

Whipple, W., Randall, C. W., Grigg, N. S., Shubinski, R. P., Grizzard, T., & Tucker, L. S. (1983). Stormwater management in urbanizing areas.

Webster, P. J., & Hoyos, C. (2004). Prediction of monsoon rainfall and river discharge on 15-30-day time scales. Bulletin of the American Meteorological Society, 85(11), 1745-1765.